Mineralogical characteristics of the heterolithic formations from the Carpathian Foredeep Miocene sediments, south-eastern Poland

Anna Przelaskowska[1], Urszula Zagórska[2], Andrzej Urbaniec[3], Grażyna Łykowska[4], Jolanta Klaja[5], Jacek Grela[6], Katarzyna Kędracka[7]

[1] *Oil and Gas Institute – National Research Institute, Krakow, Poland, e-mail: przelaskowska@inig.pl (corresponding author), ORCID ID: 0000-0003-3355-7676*
[2] *Oil and Gas Institute – National Research Institute, Krakow, Poland, e-mail: zagorska@inig.pl, ORCID ID: 0000-0002-9284-6120*
[3] *Oil and Gas Institute – National Research Institute, Krakow, Poland, e-mail: urbaniec@inig.pl, ORCID ID: 0000-0002-4717-1806*
[4] *Oil and Gas Institute – National Research Institute, Krakow, Poland, e-mail: lykowska@inig.pl, ORCID ID: 0000-0002-1201-4173*
[5] *Oil and Gas Institute – National Research Institute, Krakow, Poland, e-mail: klaja@inig.pl, ORCID ID: 0000-0003-0147-0816*
[6] *Petrogeo – Laboratory and Geological Services Company, Jasło, Poland, e-mail: grela@petrogeo.pl*
[7] *Petrogeo – Laboratory and Geological Services Company, Jasło, Poland, e-mail: kasprzyk@petrogeo.pl*

Abstract: Heterolithic complexes from the Carpathian Foredeep are a subject of growing attention as many natural gas accumulations of industrial importance have been discovered in such formations during the last decades. The aim of the presented work was to determine lithotypes of different lithology and mineralogical composition in the heterolithic sequences. Individual lithotypes were distinguished of macroscopic observations of cores, X-ray diffraction analysis (XRD) and X-ray fluorescence method (XRF). Preliminary distinction between the lithotypes was based on macroscopic observations of the core samples. Correlation plots between the contents of particular minerals (XRD analyses) and corresponding elements (XRF analyses) were used for verification of the lithotypes distinguished based on macroscopic observations. Swelling properties of the investigated rocks were determined using the cation exchange capacity (CEC) values. The following lithotypes were identified: medium- to fine-grained sandstones, fine- to very fine-grained sandstones, clayey sandstones, sand-dominated heteroliths, heteroliths with approx. equal proportions of sandstones and mudstones, mud-dominated heteroliths, mudstones, clayey shales. Such division provides a basis for precise petrophysical characterization of the analyzed profiles, that is assignment of particular petrophysical parameters values to individual lithotypes. More reliable petrophysical parameters in the geophysical interpretation of heterolithic sequences allow for a more precise determination of zones characterized by good reservoir parameters.

Keywords: Carpathian Foredeep, heteroliths, lithotypes, mineralogical composition, cation exchange capacity (CEC)

INTRODUCTION

The Carpathian Foredeep Basin (CFB) is the northern part of a huge Pannonian Basin System (PBS) developed in the Central European region (Fig. 1).

The PBS sediment series is the subject of extensive geological analysis in the aspects of conventional and unconventional reservoirs (Király et al. 2010, Badics & Vető 2012, Velić et al. 2012, Malvić et al. 2014, Bartha et al. 2018). The Carpathian Foredeep

basin is not as thoroughly recognized in terms of stratigraphy and lithology as other parts of the PBS (Nagymarosy & Muller 1988, Sacchi & Horváth 2002, Malvić 2012, Pavelić & Kovačić 2018).

The terms "heterolithic bedding" or "heterogeneous sequence" are used commonly in the description of sedimentary series that are built of interlayered packets (laminae or lenses) of sandstone, mudstone and claystone. The thicknesses

of the separate intervals corresponding to different lithologies can be various, from millimetres to decimetres (Thomas et al. 1987, Ghosh et al. 2006, Lettley & Pemberton 2015). Generally, series of such sediments are termed heteroliths. Heteroliths are not only reservoir rocks, but also source rocks that exhibit a high concentration of total organic matter (Matyasik et al. 2007, Kotarba et al. 2011).
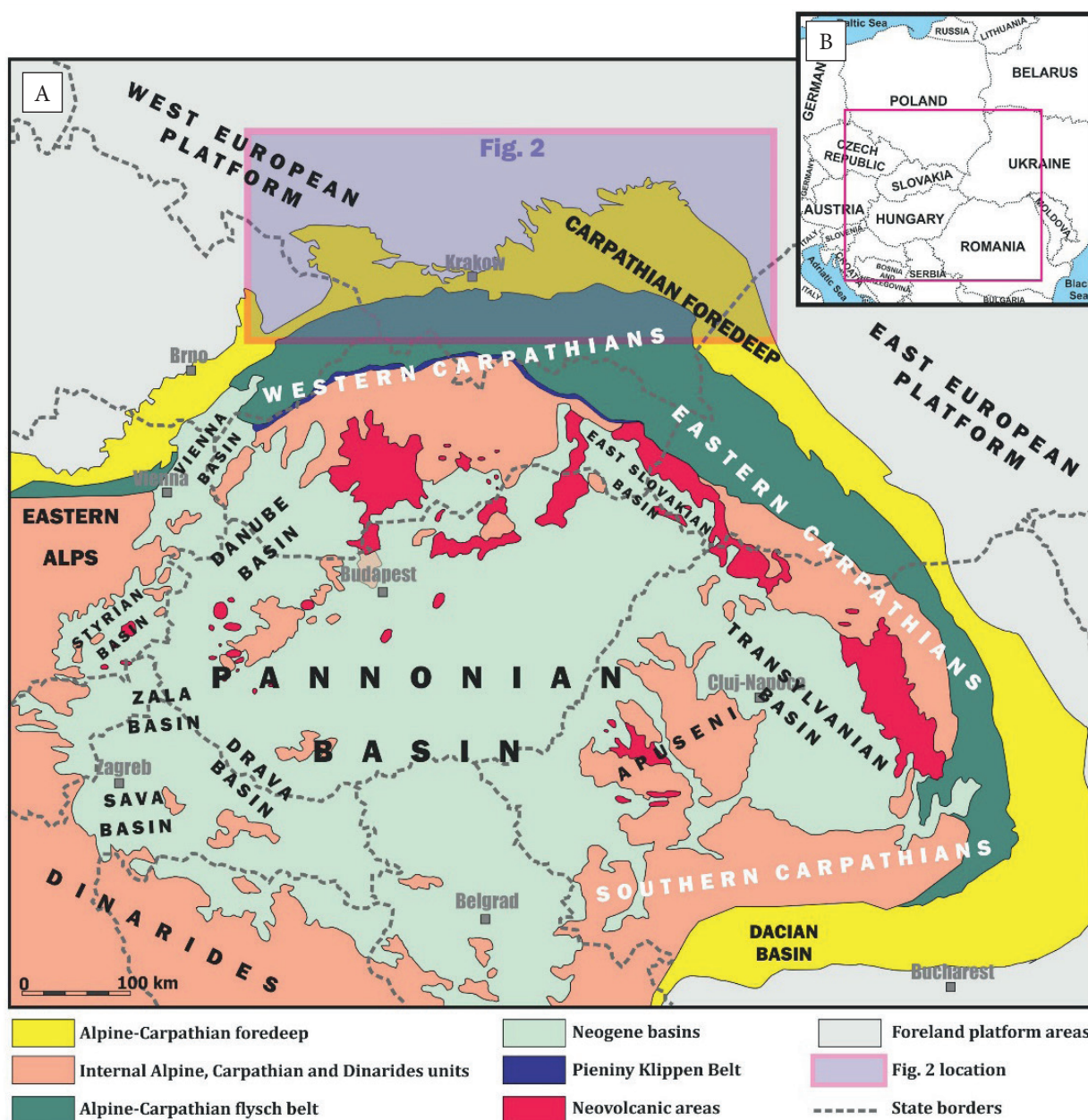

Fig. 1. *Generalized outline of Central Europe region (A); location of the study area (pink rectangle – see Fig. 2) in relation to the Carpathians and the Pannonian Basin System (PBS) (B) (after Kováč et al. 1998, Golonka et al. 2011)*

The heterogeneous sequences are commonly found in the Miocene sediment profile of the CFB. These sequences can be formed in many depositional environments and at various depths (Terwindt & Breusers 1972, Martin 2000, Jackson et al. 2005, Donselaar & Geel 2007, Łaba-Biel et al. 2020). Considering the ratio of sandstone/siltstone to mudstone/claystone, the thickness of the layers and the frequency of their appearance, various types of heterogeneous sequences can be defined. For instance, Lis & Wysocka (2012) on the basis of well data analysis defined in the Carpathian Foredeep area three main types of heterogeneous sequences:

1) dominated by mudstone,
2) with an approximately equal proportion of sandstone/siltstone and mudstone,
3) dominated by sandstone and siltstone.

The specific types of bedding are characteristic of the heterogeneous sequence, predominantly flaser, wavy and lenticular laminations that are created by the interchanging deposition from traction and suspension. During the traction-based sedimentation, sand and silt fractions with small-scale cross-bedding or planar bedding dominate. The suspension-based sedimentation favours the deposition of mudstone and claystone without lamination, as well as flaser, wavy or lenticular laminations.

Increasing attention given to heterolithic complexes from the Carpathian Foredeep is related to the fact that many natural gas accumulations of industrial importance have been discovered in such complexes during the last decades (vide Myśliwiec 2004, Myśliwiec et al. 2004). The reservoirs occurring in such rocks are referred to as a subconventional hybrid system, in which reservoir rocks of both unconventional (mainly mud-dominated rocks) and conventional (subordinate sandstones) nature are present (Poprawa et al. 2018). Gas inflows are often obtained from intervals with low porosity and permeability, which, according to well log interpretation, are characterized by relatively low gas saturations. Heterolithic complexes generally pose a major interpretive problem because of the low resolution of standard geophysical measurements and the high value of calculated mean saturations.

Heterolithic formations, in the context of evaluation of their petrophysical properties, are therefore a challenge both from the point of view of laboratory measurements and correct interpretation of borehole measurements.

The presented work is a part of a broader project aimed at "Development of a new methodology of laboratory measurements and geophysical data interpretation for the heterolithic formations of the Carpathian Foredeep Miocene" (Klaja 2019). Routine sampling procedure for petrophysical measurements on cores may not always accurately determine the average reservoir properties in the case of heterolithes. Selection of samples reflecting particular lithotypes is of vital importance for determining average reservoir properties. The aim of the work was to distinguish lithotypes of different lithology and mineralogical composition in the heterolithic sequences of autochthonous Miocene. Such division enabled allocation of the measured in the next step of the project (Klaja 2019) petrophysical parameters to particular lithotypes. Well-grounded average petrophysical parameters in the geophysical interpretation of the heterolithic sequence allow for a more precise determination of zones/intervals with better reservoir parameters and increased probability of hydrocarbon saturation. Individual lithotypes were distinguished and characterized with the use of the following methods: macroscopic observations of cores, XRD and XRF measurements, microscopic observations and cation exchange capacity (CEC) measurements.

GEOLOGICAL BACKGROUND

The study area is located in southern Poland within the eastern part of the Carpathian Foredeep area and in the marginal part of the Outer Carpathians. Three minor zones: Sędziszów (called in this article as "S"), Tyczyn ("T") and Pantalowice ("P") define the whole study area (Fig. 2).

In the vertical section of the research area five structural stages can be distinguished. The oldest structural stage is represented by a series of Neoproterozoic anchimetamorphic rocks of the Ediacaran age.
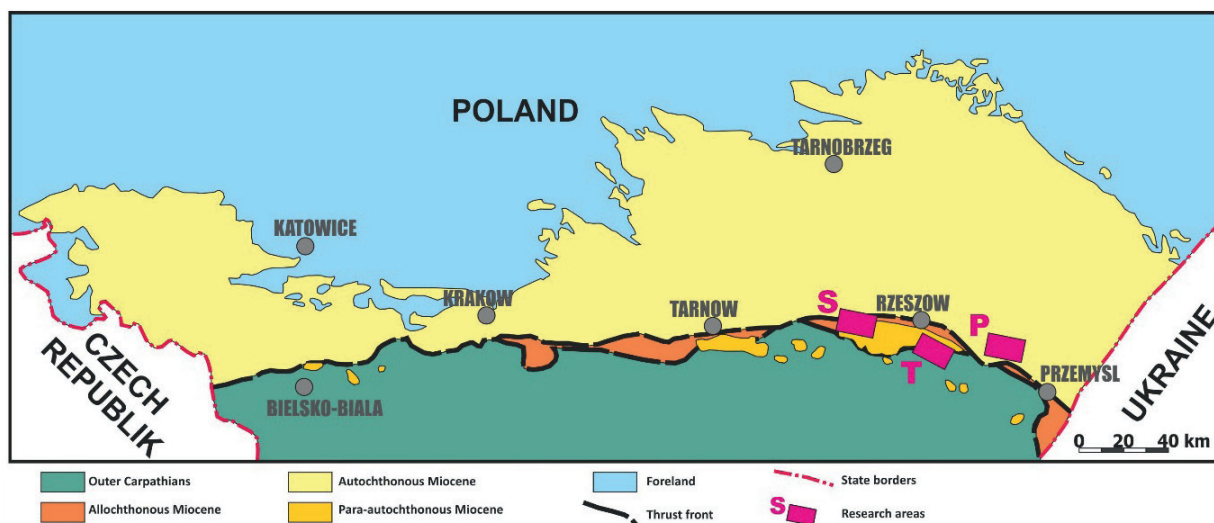
Fig. 2. *Location of the research area against the range of the Carpathian Foredeep in Poland; ranges of geological units according to Porębski & Warchoł (2006)*

The next stage is composed of Meso-Paleozoic rock complex characterized by strongly diversified thicknesses (from 0 up to 2000 m) and lithology (Moryc 1992, 1996, Maksym et al. 2001, Urbaniec et al. 2019, 2020). In the eastern part of the research area (zone P) the Ediacaran sediments are covered directly by Miocene series.

The younger structural stage is formed by the autochthonous Miocene formations (Badenian-Sarmatian), which were initially deposited in the CFB. The sedimentary basin of the Carpathian Foredeep was a fragment of a large foreland graben basin stretching along the whole Carpathian arc (Fig. 1). The complex of autochthonous Miocene strata in the research area can be divided into three main units: the Lower Badenian clastic series, the Upper Badenian evaporite series and the Upper Badenian-Sarmatian clastic series (Jasionowski 1997, Oszczypko et al. 2006, Urbaniec et al. 2019). The siliciclastic sediments from the third mentioned lithostratigraphic unit, classified as the Machów Formation (Alexandrowicz et al. 1982, Jasionowski 1997), are an essential part of the autochthonous Miocene profile in the analyzed region of the Carpathian Foredeep. This formation manifests significant lithofacial diversity. A detailed analysis of the heterolithic parts of the Machów Formation profiles in the three

mentioned zones (see Fig. 2) is the main subject of this article.

The next structural stage consists of the Miocene-age deformed sediments situated directly in front of the Carpathian orogen (the Zgłobice unit). Finally, the highest structural stage is represented by allochthonous formations belonging to the Outer Carpathians (Golonka & Picha 2006, Oszczypko 2006, Jankowski et al. 2012, Jankowski 2015) (Figs. 1, 2).

MATERIALS AND METHODS

Drill core material

The selected core material was collected during the realization of the mentioned above project (Klaja 2019). Samples represent various types of heterolithic rocks from different parts of Miocene profile (depending on zone) however, all analyzed core intervals belong to the Machów Formation. The investigations were carried out on core material (102 samples) from five boreholes located in three zones (Fig. 2):

1) zone S; wells: S-33K, S-34; depth interval: 2210–2560 m;
2) zone T; wells: T-1, T-2K; depth interval: 2830–3370 m;
3) zone P; well P-7K; depth interval: 1040–1070 m.

Boreholes from the S zone are located in area of known multi-horizon gas reservoir. The core material from this zone belongs to the deeper part of Miocene profile, below gas-bearing horizons. In contrast to the upper part of Miocene profile, the analyzed interval is dominated by fine-grained formations of little lithological variability. The core material consists mostly of mudstones and mud-dominated heteroliths, regularly interlayered with sandstone layers of 1 to 3 cm in thickness. Only occasionally thin interlayers of fine-grained sandstone with planar, flaser, wavy and sometimes convolute lamination can be found. These formations should be classified as the lower complex of fine-grained sediments *sensu* Krzywiec et al. (2008).

The T zone is characterized by relatively high thickness of autochthonous Miocene formations (up to 800 m), overlayered by tectonically deformed Miocene sediments belonging to the Zgłobice unit and Outer Carpathians units. The core material from this zone shows a high lithological diversity. Apart from heterolithic and mudstone series, thick (up to 2 m) beds of fine-grained sandstones with lenticular, wavy, and in places, convolute lamination were found.

The analyzed well from the P area is located in a multi-horizon gas reservoir developed in fine-grained sandstones and mudstones. More than 10 gas-bearing horizons have been recognized in the field. The data from wells show a tripartite character of autochthonous Miocene profile in this zone, resulting from lithological differentiation (Rzemieniarz & Ratuszniak 2008). The upper part of the profile, up to the depth of about 1000 m, is built of alternating sandstone or sandstone-mudstone complexes, with overlaying clayey-mudstone sediments. The middle part of the profile (covering generally the interval 1000–1550 m) is dominated by fine-grained sediments. The lower part of the profile (below the depth of 1550 m) is characterized by strongly differentiated lithology, with sandstone and mudstone horizons of larger thickness separated by mudstone and claystone series. The investigations were conducted on samples from one 18 m long core of fine-grained sediments from the middle part of the Miocene profile. This core is dominated by thinly laminated, mud-dominated heteroliths, while heteroliths with an approximately equal proportion of sandstone/siltstone and mudstone are much less common. According to the lithofacies division of the Miocene, proposed by Krzywiec et al. (2008), these formations belong most probably to the interdeltaic complex.

The samples were selected in such a way as to reflect the lithological diversity of the studied formations as much as possible in order to investigate all the possible lithotypes.

Laboratory measurements

The distinction of particular lithotypes was carried out basing on macroscopic observations, analyses of mineral (XRD) and chemical (XRF) composition, and petrographic studies in optical and scanning microscopy. In addition, CEC cation exchange capacity was measured to determine the swelling capacity of the studied rocks.

XRD measurements were conducted with the use of Panalytical X'Pert Pro apparatus with modern ultra-fast detector (real time ultra-strip X'Celerator). Quantitative mineral composition was calculated by the Rietveld method with the use of the SIROQUANT software, which is useful for analysing samples containing clay minerals (Kowalska 2013). Measurements of the separated clay fraction were carried out on sedimented slides in both air-dried (AD) and glycolated conditions (GY). Detailed identification of the illitic material was made on preparations from the <0.2 m fraction using diagrams by Środoń (Środoń 1980, 1981, 1984, Dudek & Środoń 1996). The chemical composition measurements were made with a portable X-ray fluorescence spectrometer (pXRF) S1 TITAN, Bruker. Petrographic observations on thin sections were carried out using an AXIOPLAN CARL ZEISS OPTON polarizing microscope. The investigated samples were described based on Picard (1971) and Pettijohn et al. (1972) clastic rock classifications. SEM analysis was conducted using JSM 6300 Jeol scanning electron microscope coupled with OXFORD INSTRUMENTS X-ray microanalyzer EDS (Energy Dispersive Spectroscopy. Cation Exchange capacity

was determined using the cobalt hexaamine spectrophotometric method (Bardon 1983, AFNOR NFX31-130 1999, Przelaskowska & Klaja 2014). Measurements were conducted using a Shimadzu UV-1280 spectrophotometer at 470 nm wavelength.

Procedure applied to distinguish particular lithotypes

Preliminary distinction of the lithotypes based on macroscopic observations of the core samples

The investigated material consists of "pure" lithotypes, i.e., sandstones of various grain sizes, mudstones and clayey shales, and "mixed" lithotypes – heteroliths. Heterolithic lithotypes from the point of view of rock classification are a mixture of sandstones, siltstones, mudstones and claystones in different proportions. Due to the thin-layered nature of the analyzed rocks, the individual lithologies cannot be separated in petrophysical studies conducted on inch cores. Therefore, lithotypes with varying proportions of sandstone and mudstone were introduced. Lithotypes were determined from 3.0–3.5 cm long inch cores prepared for petrophysical measurements and corresponding core fragments were sampled for petrographic and mineralogical investigations. Heterolithic lithotypes: sand-dominated heteroliths, heteroliths with approx. equal proportions of both lithologies and mud-dominated heteroliths were distinguished by estimating the amount of sandstone and mudstone laminae in the core fragment studied. A sample heterolith with approx. equal proportions of sandstone and mudstone is shown on Figure 3.

Correlation plots between the contents of particular minerals (XRD analyses) and corresponding elements (XRF analyses)

Plots of minerals vs. corresponding elements are routinely used in INiG-PIB to verify quantitative X-ray analysis results. They are also adopted in chemostratigraphy studies to establish and verify the mineralogical affinity of elements used in the chemostratigraphic divisions (Craigie 2018). The diagrams constructed in the presented work were used for verification of the lithotypes distinguished on the basis of macroscopic observations. The applied correlation relationships are shown in Table 1.

Table 1
Applied correlations of minerals vs. corresponding elements

Mineral content	Element content
Sum of quartz and feldspars	SiO_2
Sum of clay minerals	Al_2O_3
Sum of carbonates (calcite, dolomite, ankerite)	CaO
Sum of K feldspars, micas and illitic minerals	K_2O

Fig. 3. An example of a heterolith from the T zone with approx. equal proportions of sandstone and mudstone

The analyses were conducted for all samples jointly, and then samples from each of the zones were separated on the plots by different marks. Therefore, the obtained plots illustrate not only the differences between particular lithotypes, but also take into account the regional variation within each lithotype (Figs. 4–6).

Analysis of the variability of parameters estimated by XRD measurements

Mineralogical characterization of the separated lithotypes was based on the XRD measurements. The analysis of parameters that most differentiate the individual lithotypes, such as clay and quartz contents, enabled verification of the problematic samples e.g., very fine-grained sandstone/mudstone allocation. Investigations of the separated clay fraction allowed for precise identification of clay minerals.

Optical microscope and SEM studies

Due to a small area of observation and the difference in scale in relation to the size of the sample selected for petrophysical research the microscopic studies were not a decisive method for assigning samples to particular lithotypes. They were used for verification of the division based on macroscopic observations and XRD/XRF plots, and for more detailed characterization of the distinguished lithotypes.

RESULTS

Based on macroscopic observations the following lithotypes were distinguished among the studied rocks:
– medium- to fine-grained sandstones (**Ss_m**),
– fine- to very fine-grained sandstones (**Ss_f**),
– clayey sandstones (**Ss_cl**),
– sand-dominated heteroliths (**Ht_s**),
– heteroliths with approx. equal proportions of both lithologies (**Ht_sm**),
– mud-dominated heteroliths (**Ht_m**),
– mudstones (**Ms**),
– clayey shales (**Cs**).

Not all of the lithotypes were present in every zone (Tab. 2). Only fine- and very fine-grained sandstones, mud-dominated heteroliths and mudstones were found in all zones (Tab. 2). The most widespread lithotype in the studied sediments is represented by mud-dominated heteroliths (Tab. 2), although the proportions of sandstone and mudstone layers vary between particular zones. The S region sediments are characterized mainly by mud-dominated heteroliths and massive, compacted mudstones with thin inserts of fine-grained sandstone. Locally also thicker (more than 10 cm) inserts of fine- and medium-grained sandstones with parameters similar to those of conventional reservoir sandstones are found. Rocks from the T region include mud-dominated heteroliths often interlayered with thicker sandstone inserts (about 5 cm), clayey-mudstone deposits and massive mudstones locally interlayered with thicker sandstone inserts (about 5 cm). Typical heterolithic formations: mud-dominated heteroliths with densely distributed, thin sandstone laminae (order of millimetre size) occur in the P region.

Table 2
Lithotypes distinguished in the investigated zones

Lihtotype	Number of samples		
	S	**T**	**P**
Ss_m	3	6	–
Ss_f	6	14	1
Ss_cl	7	–	–
Ht_s	–	4	2
Ht_sm	–	7	–
Ht_m	2	4	13
Ms	5	18	4
Cs	1	5	–

Explanations: S, T, P – zones, Ss_m – medium- to fine-grained sandstones, Ss_f – fine- to very fine-grained sandstones, Ss_cl – clayey sandstones, Ht_s – sand-dominated heteroliths, Ht_sm – heteroliths with approx. equal proportions of both lithologies, Ht_m – mud-dominated heteroliths, Ms – mudstones, Cs – clayey shales.

Correlation diagrams

Groups of samples corresponding to the described above lithotypes can be clearly distinguished based on correlation diagrams representing mineral (XRD) and chemical (XRF) composition. The distinction is based on such parameters as: sum of quartz and feldspar vs. SiO_2, sum of mica and potassium feldspar vs. K_2O and sum of clay minerals vs. Al_2O_3 (Figs. 4–6). No relationship was observed between carbonate content and particular lithotypes (Fig. 7).
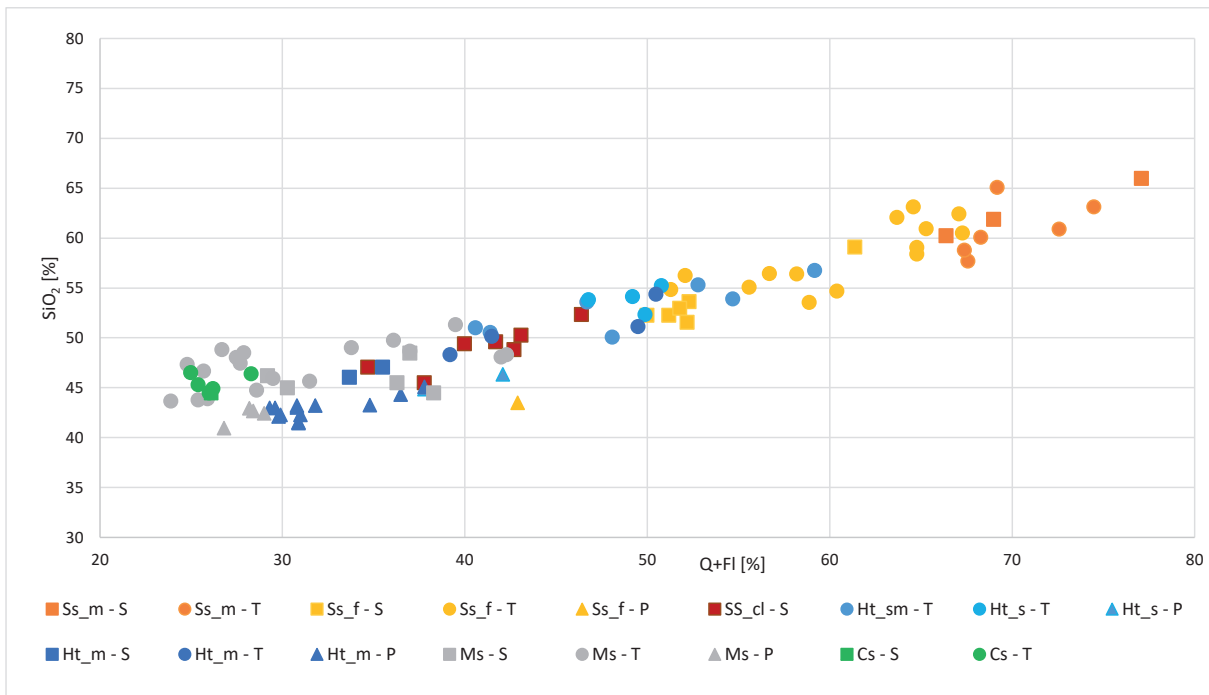
Fig. 4. *Correlation between silicon dioxide (SiO_2) and sum of quartz and feldspars (Q+Fl): Q – quartz, Fl – feldspars; S – Sędziszów zone, T – Tyczyn zone, P – Pantalowice zone*
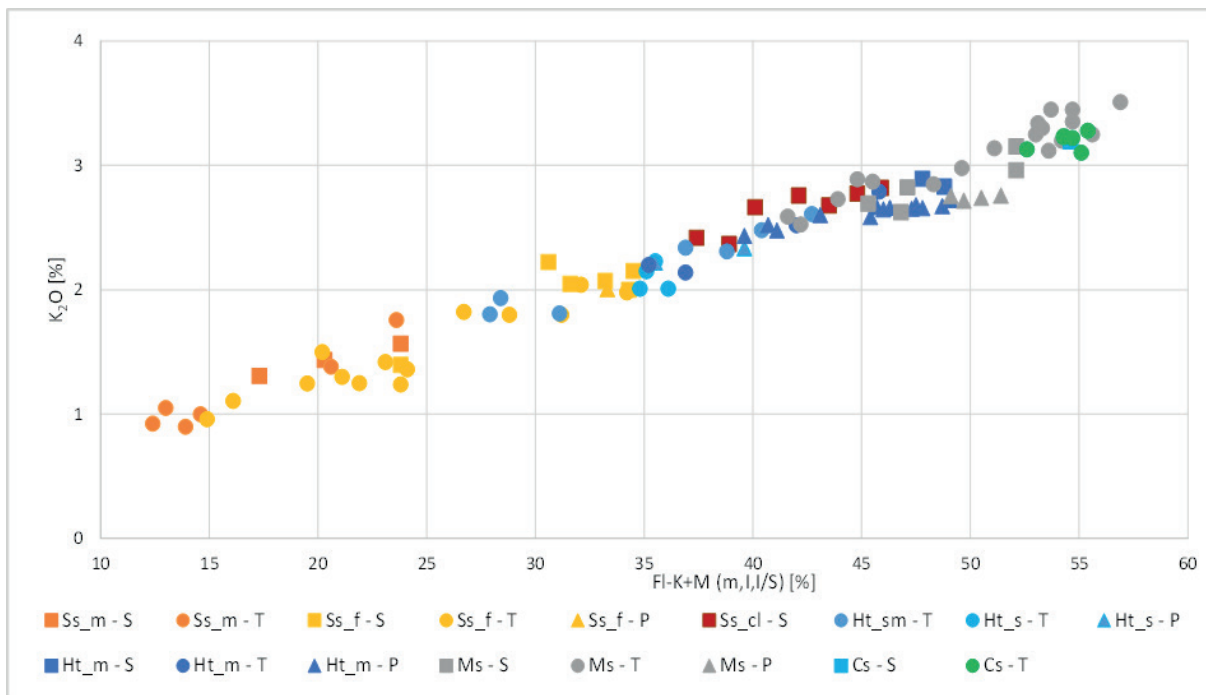

Fig. 5. *Correlation between potassium oxide (K_2O) and sum of K feldspars, micas and illitic minerals (Fl-K, M): M – micas and illitic minerals, m – micas, I – illite, I/S – mixed-layer mineral illite-smectite; S – Sędziszów zone, T – Tyczyn zone, P – Pantalowice zone*
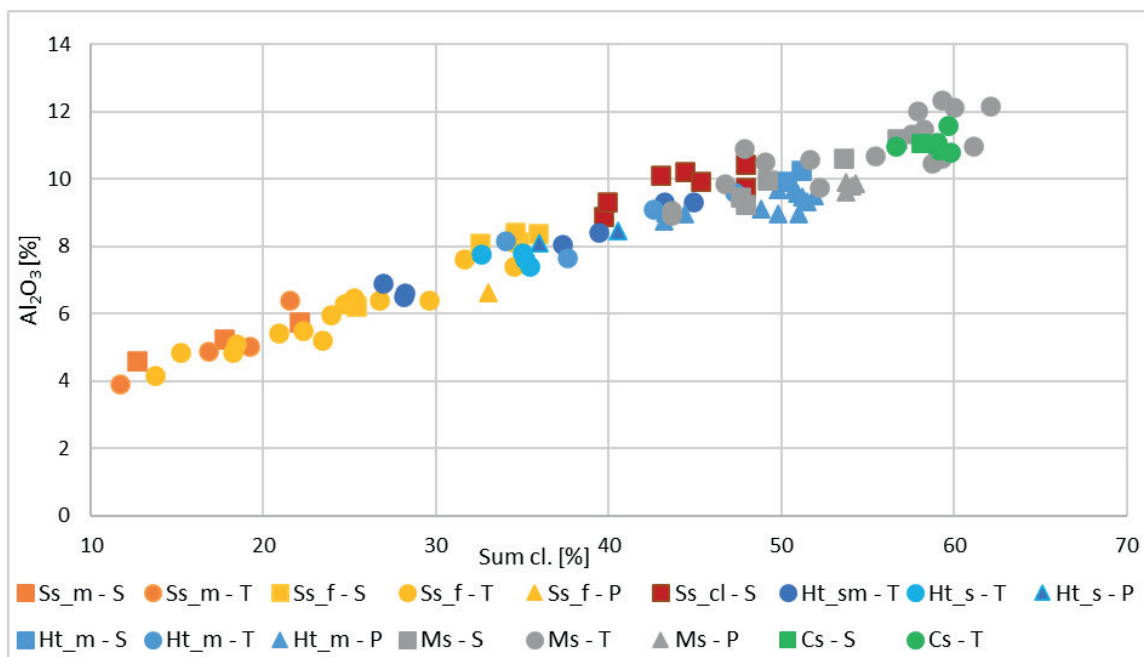
Fig. 6. Correlation between aluminium oxide (Al₂O₃) and sum of clays (sum Cl): S – Sędziszów zone, T – Tyczyn zone, P – Pantalowice zone
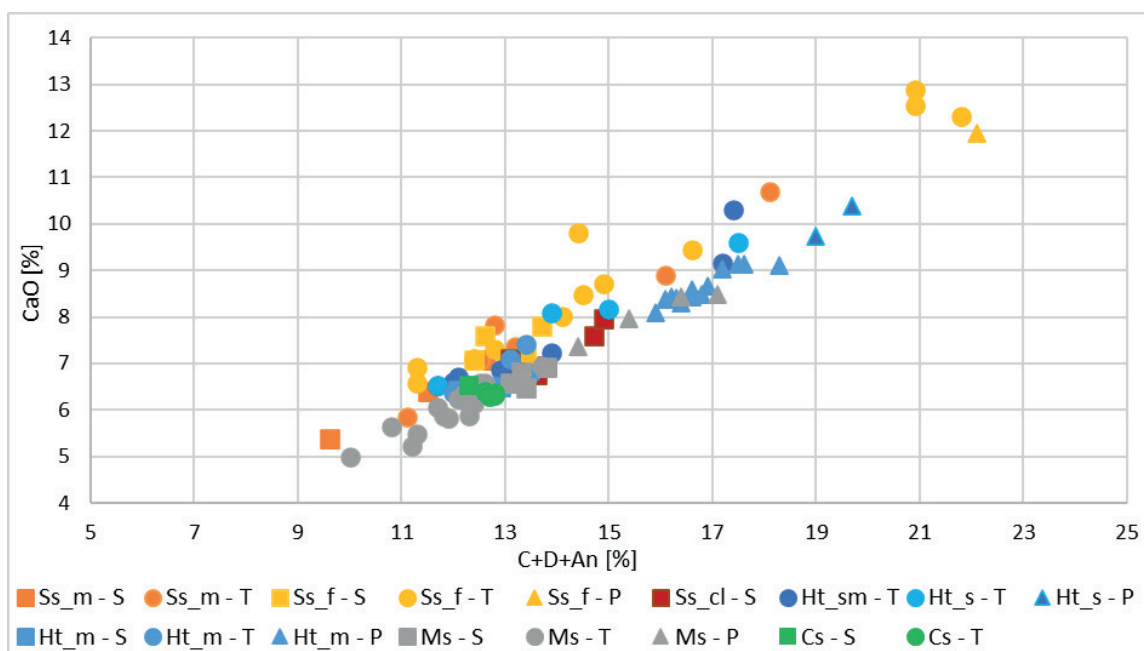

Fig. 7. Correlation between calcium oxide (CaO) and sum of carbonates (C+D+An): C – calcite, D – dolomite, An – ankerite; S – Sędziszów zone, T – Tyczyn zone, P – Pantalowice zone

The boundary between sandstones from the S and T zones and fine-grained rocks (mudstones, clayey-shales and most of heteroliths) is very clearly marked on the diagrams. This boundary is marked by contents of about 50% quartz and feldspar (Fig. 4), 30% of the sum of potassium feldspar

and micas (Fig. 5) and 36% of clay minerals (Fig. 6). Some differentiation between sandstones from the two zones is also evident. Rocks from the S zone are characterized by slightly lower amounts of quartz, and higher clay content than samples from the T zone. Mudstones from all three zones are characterized by a quartz content smaller than 43% (Fig. 4) and sum of clays exceeding 43% (Fig. 6). Heteroliths form an intermediate group of samples. Heteroliths from the T zone plot mostly between the sandstone and mudstone areas on the quartz content diagram (Fig. 4). Only a few samples of Ht_sm overlap with sandstones with the lowest amount of quartz and the highest clay content (Fig. 4). Ht_m from the S and P zones occur in the mudstone area (Figs. 4–6).

Ss_cl from the S zone are placed partly in the mudstone area and partly between sandstones and mudstones (Figs. 4–6). Cs are present in the area of mudstones with the highest clay and lowest quartz content (Figs. 4–6).

Petrographic characterization of the distinguished lithotypes

Description of each lithotype was based on macroscopic examination of cores, XRD and XRF results, optical and scanning microscopy observations and CEC measurements. Macroscopic images of core fragments (section A), optical microscope images (section B) and SEM images (section C) for each lithotype are presented on Figures 8–16.
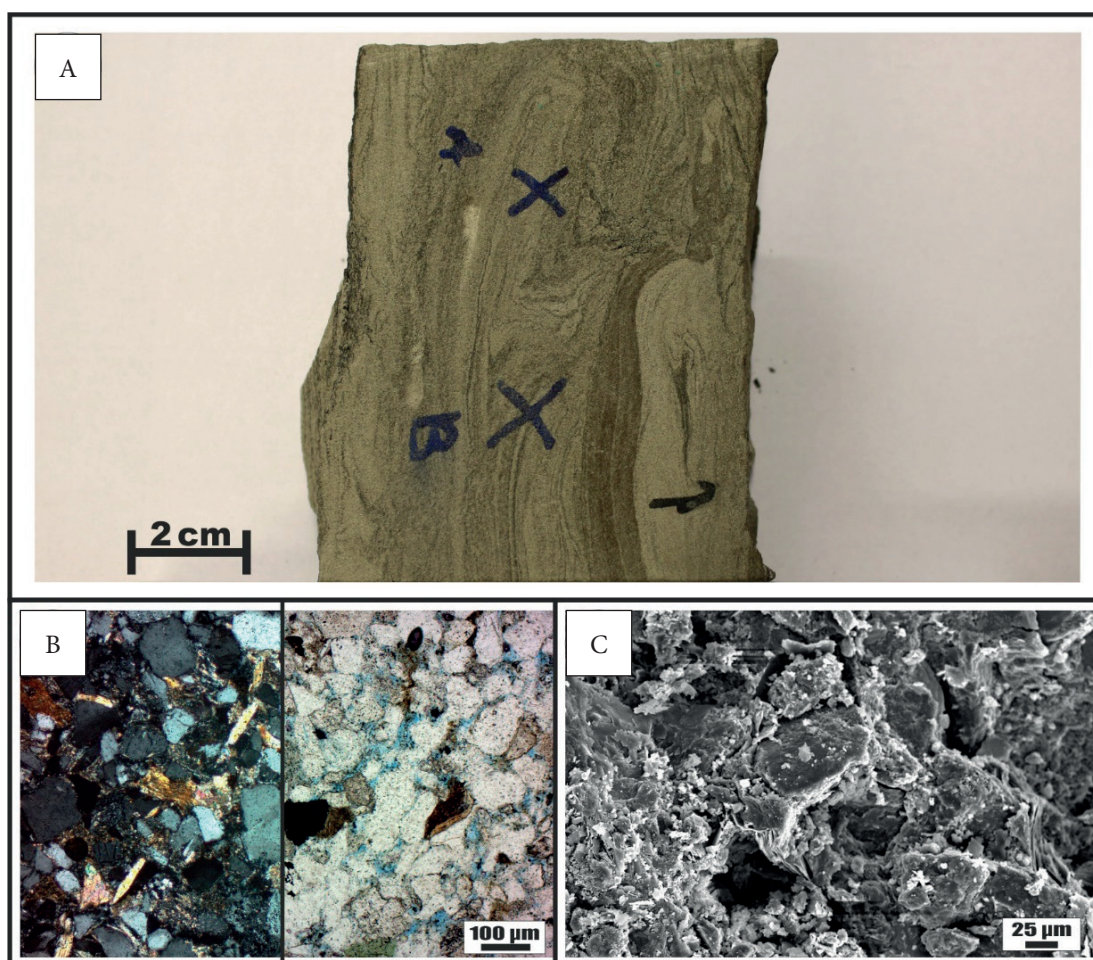

Fig. 8. *Medium- to fine-grained, laminated sandstone from the S zone, lamination accentuated by organic matter (A); subarcose arenite with carbonate-clay matrix (B – left); interparticle pores visible on a thin section impregnated with blue epoxy resin (B – right); pore space filled with clay minerals, micrite, dolomicrite, and fine-crystalline silica, numerous interparticle fine pores visible (C)*
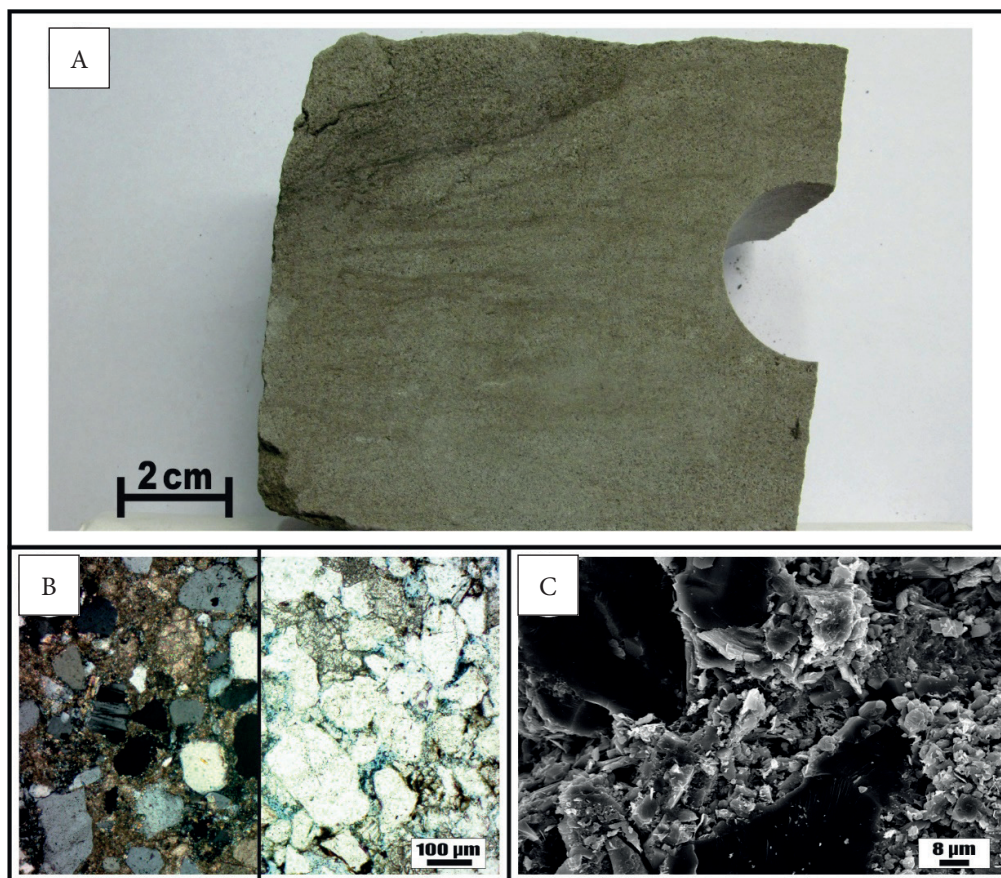
Fig. 9. *Medium- to fine-grained, massive sandstone from the T area (A); subarkose arenite with carbonate-clay matrix (B – left); interparticle pores visible in a thin section impregnated with blue epoxy resin (B – right); pore space filled with carbonates (calcite and dolomite), clay minerals and fine-crystalline silica, numerous interparticle micro- and nanopores visible (C)*

Medium- to fine-grained sandstones (Ss_m)

Medium- to fine-grained sandstones are found in S and T zones. Two types of these rocks can be distinguished:

1) Light grey sandstones, with planar, flaser and wavy lamination accentuated by organic matter (Fig. 8A). Microscopically described as well to moderately sorted subarcose arenites, locally with inserts of subarcose wackes, with carbonate-clay matrix (Fig. 8B – left). Interparticle pores are visible both in optical microscope (on a thin section impregnated with blue epoxy resin; Fig. 8B – right) and on SEM image (Fig. 8C).

2) Light grey mostly massive sandstones (Fig. 9A). Microscopically described as well-sorted quartz arenites with carbonate-clay matrix (Fig. 9B – left). Zones with higher pore accumulation are visible on a thin section impregnated with blue epoxy resin (Fig. 9B – right). Intraparticle micro- and nanopores were observed in the SEM image (Fig. 9C).

Fine- to very fine-grained sandstones (Ss_f)

Ss_f lithotype is one of the most numerous and occurs mainly in S and T zones (Tab. 2). It is represented by light grey sandstones with different types of lamination (planar, flaser, wavy and lenticular) of darker material (Fig. 10A). Microscopically described as subarcose arenites and, in a few cases, mudstones/siltstones with carbonate-clay matrix and a planar structure accentuated by the arrangement muscovite plates, clay minerals and strips of organic matter (Fig. 10B – left). SEM images show intraparticle micro and nanopores connected with clay aggregates; the number of intergranular micropores is strongly limited (Fig. 10C).
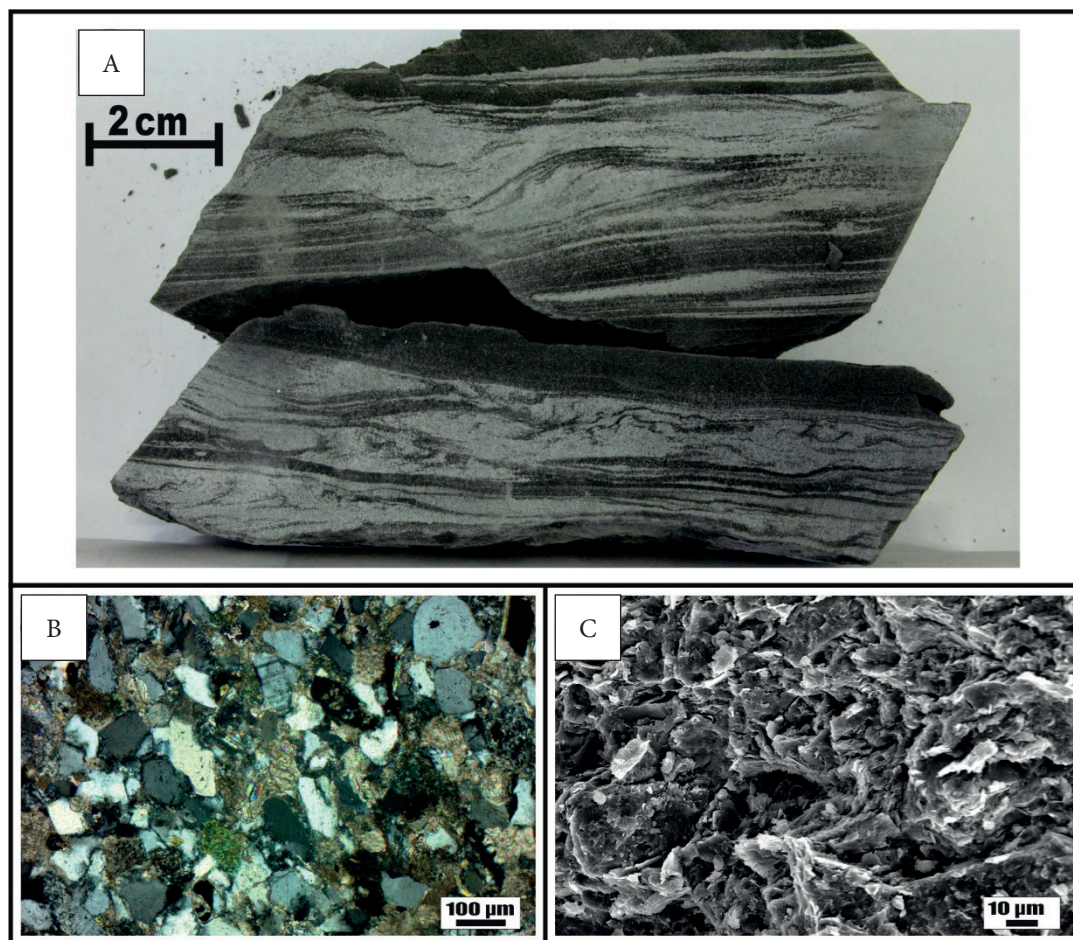
Fig. 10. *Fine-grained sandstone from the T zone with planar, flaser and wavy lamination (A); subarkose arenite with carbonate-clay matrix (B); intraparticle micro- and nanopores connected with clay aggregates (C)*

Clayey sandstones (Ss_cl)

Ss_cl lithotype occurs only in the S zone (Tab. 2). These rocks are dark grey very fine-grained sandstones, in most cases displaying poorly visible planar lamination (Fig. 11A). Microscopically described as very fine-grained rocks with a planar structure accentuated by the arrangement of muscovite plates and clay minerals (Fig. 11B). Optical microscopy revealed no pore spaces, while SEM images show intraparticle micro and nanopores connected with clay aggregates (Fig. 11C).

Sand-dominated heteroliths (Ht_s)

Ht_s lithotype occurs in T and P zones. The sandstone layers display wavy lamination (Fig. 12A). Microscopically described as subarcose arenites/wackes with carbonate-clay matrix and a planar

structure accentuated by the arrangement of muscovite plates (Fig. 12B), characterized by a lack of intergranular pore spaces. Very small amounts of nano- and micropores are visible in the SEM image (Fig. 12C).

Heteroliths with approx. equal proportions of sandstone and mudstone (Ht_sm)

Ht_sm lithotype occurs only in the T zone. Planar, flaser and wavy and lamination is clearly visible in the sandstone part, the mudstone part locally contains thin parallel sandstone laminae (Fig. 13A). Microscopically they are described as quartz wackes/mudstones with carbonate-clay matrix (Fig. 13B). Optical microscopy revealed no pore spaces, while SEM images show numerous intraparticle micro and nanopores connected with clay aggregates (Fig. 13C).
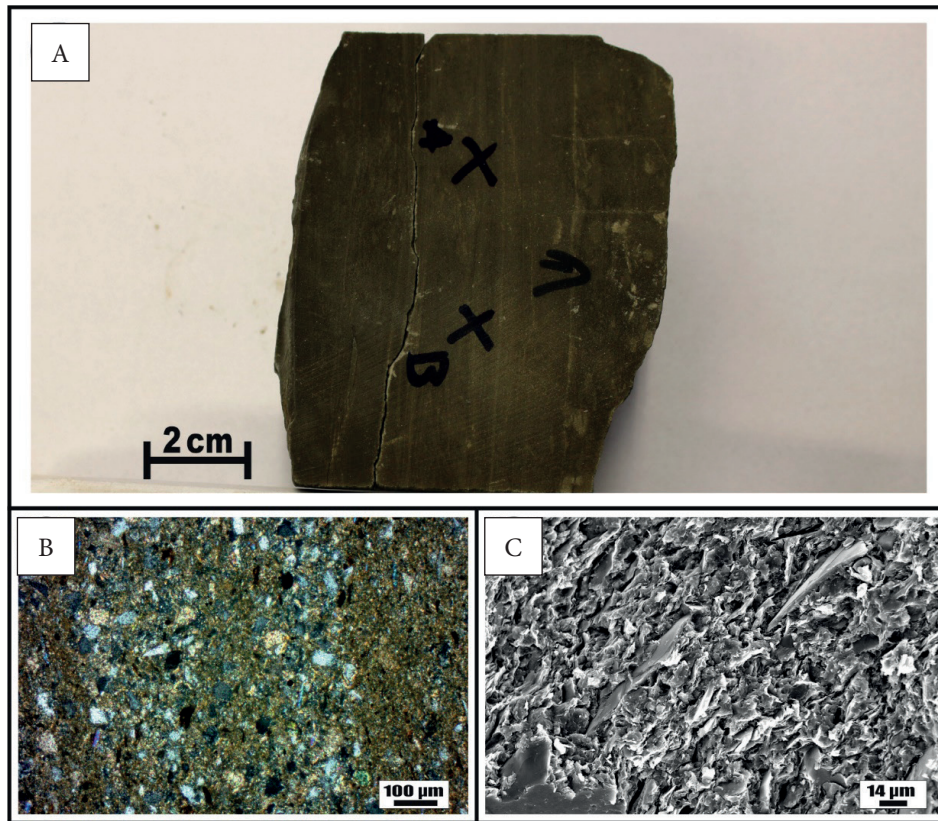
Fig. 11. *Clayey, laminated sandstone from the S area (A); fine-grained rock with planar lamination (B); lamination accentuated by the alignment of clay minerals and muscovite grains, elongated intraparticle micro- and nanopores connected with clay aggregates (C)*
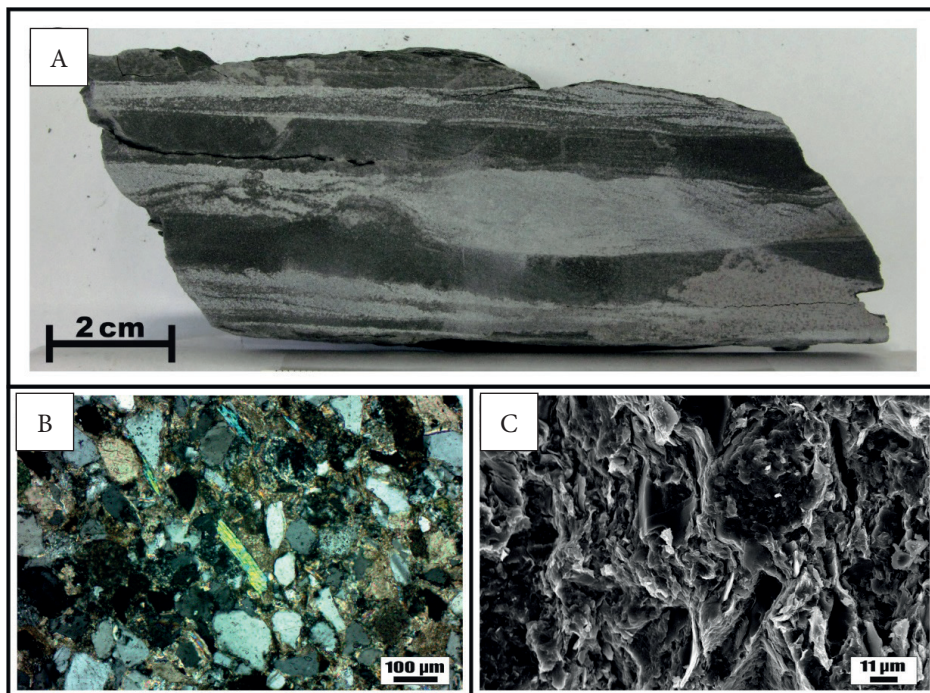

Fig. 12. *Ht_s from the T zone with wavy lamination (A); subarkose arenite/subarkose wacke with clay-carbonate matrix (B); intraparticle micro- and nanopores connected with clay aggregates (C)*
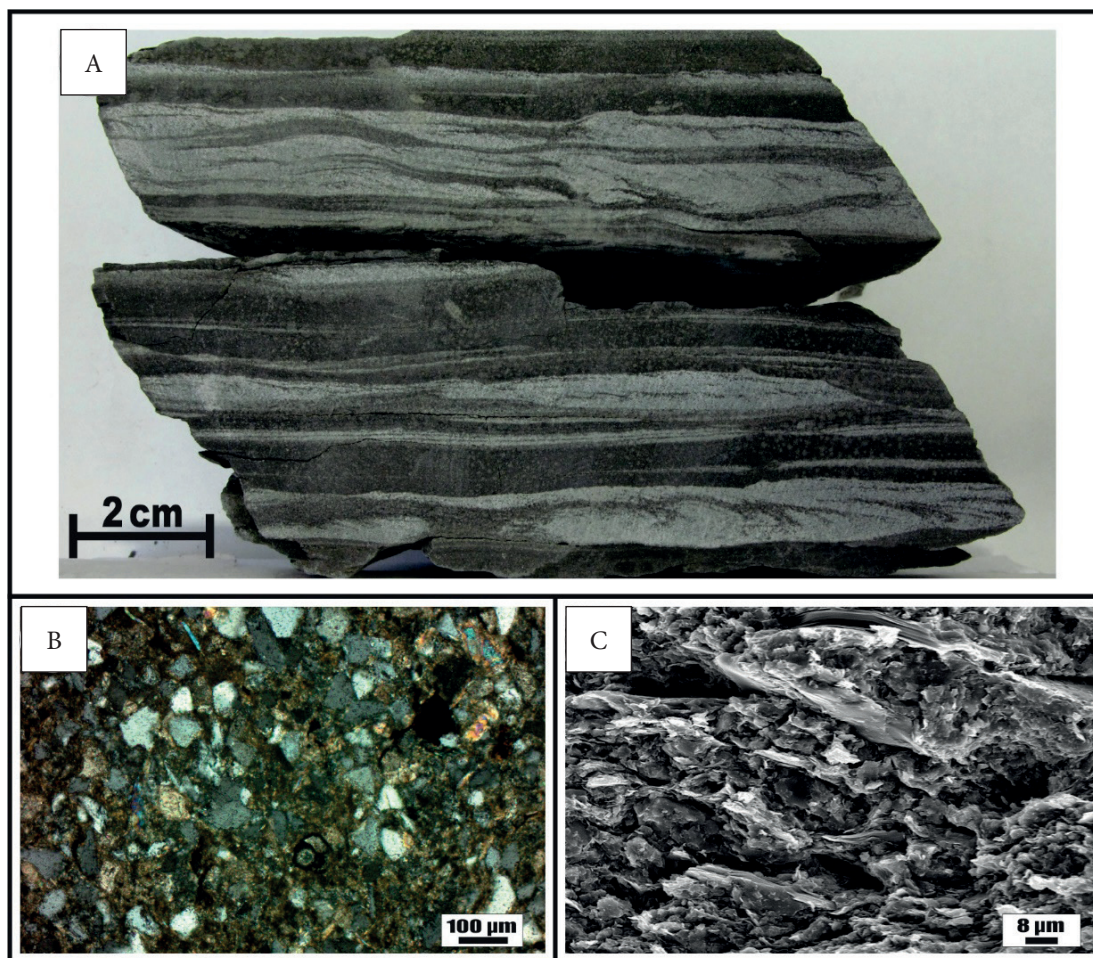
Fig. 13. *Ht_sm from the T zone, with planar and wavy lamination in the sandstone part and thin laminae of sandstone in the mudstone part (A); quartz wacke with carbonate-clay matrix/mudstone (B); intraparticle micro- and nanopores connected with clay aggregates (C)*

Mud-dominated heteroliths (Ht_m)

Ht_m lithotype is one of the most numerous and occurs in all three zones (Tab. 2). It is represented by dark grey mudstones with light grey sandstone laminae of thickness up to 5 mm, the thinnest sandstone layers (0.5–2.0 mm) can be found in samples from the P zone (Fig. 14A). Microscopically, these rocks are described as interlayers of claystone, mudstone, siltstone and subarcose wackes. They are characterized by a planar structure accentuated by layers of the above mentioned lithologies, arrangement of muscovite plates and organic matter strips (Fig. 14B). Single pores are visible locally in the sandstone layers. The SEM image shows a compact rock structure with tightly packed plates of micas and clay minerals, and infrequent micropores additionally sealed by fine crystalline carbonates represented by calcite and, to a lesser extent, dolomite (Fig. 14C).

Mudstones (Ms)

Dark grey mudstones (Fig. 15A) are the most numerous group of the investigated samples (Tab. 2). Microscopically, they are described as mudstones and claystones consisting of 70–90% carbonate-clay mass, with no free pore spaces (Fig. 15B). They are characterized by an ordered layered structure, emphasized by clay minerals and muscovite plates arrangement. SEM images show numerous intraparticle nano- and micropores associated with clay aggregates (Fig. 15C).
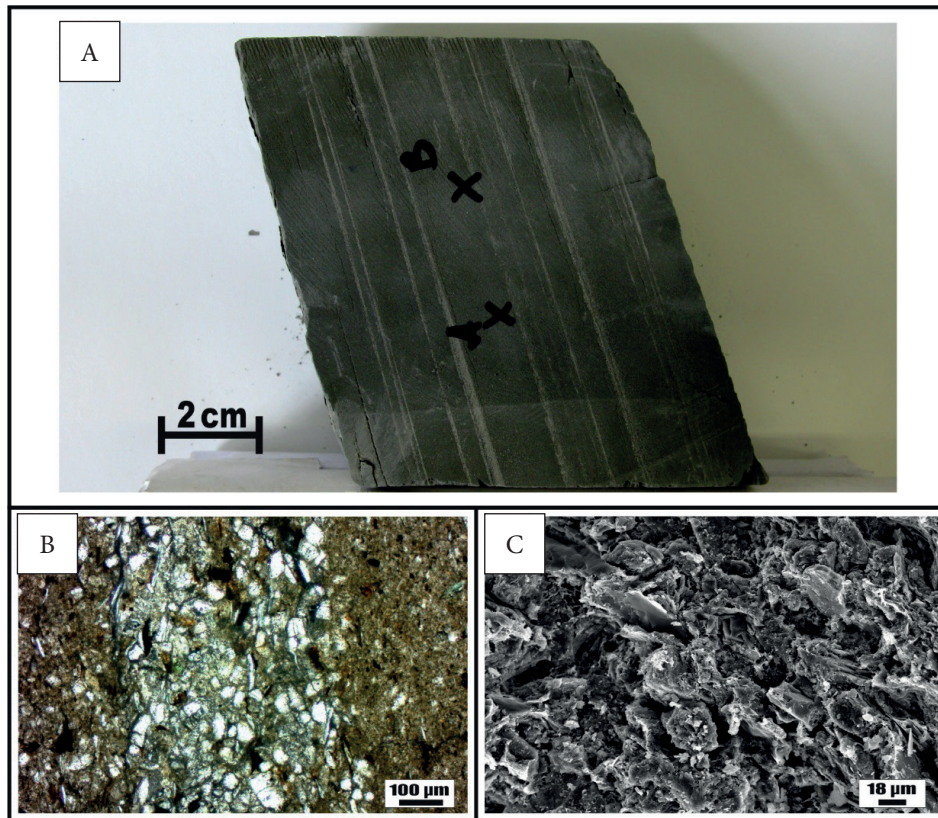
Fig. 14. *Ht_m from the P zone, with planar lamination (A); mudstone/siltstone with planar lamination accentuated by muscovite plates and organic matter (B); the number of micro- and nanopores reduced by fine crystalline carbonates (C)*

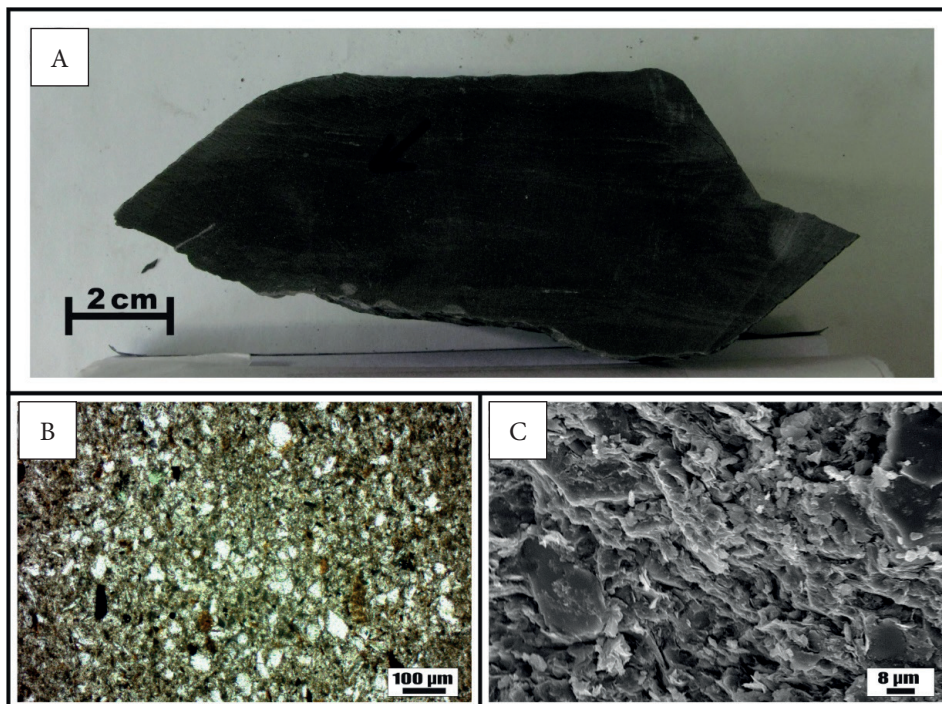
Fig. 15. *Mudstone from the T area (A); mudstone/claystone with planar lamination accentuated by clay minerals, muscovite plates and organic matter (B); numerous elongated intraparticle micro- and nanopores connected with clay aggregates (C)*

Clayey shales (Cs)

Samples representing this lithotype occur mostly in the T zone (Tab. 2). They show distinct shale fissility (Fig. 16A), a more compact material is present only locally in form of lenses (Fig. 16A). Microscopically, these rocks are described as claystones consisting of 90–95% carbonate-clay mass, with no free pore spaces (Fig. 16B). They are characterized by a planar structure, emphasized by clay minerals and muscovite plates arrangement. The planar structure and elongated intraparticle nano- and micropores associated with clay mineral aggregates are visible in the SEM image (Fig. 16C).

Mineralogy and swelling properties

The average contents of the major minerals (quartz, clay minerals and carbonates) and values of the cation exchange capacity (CEC) of the studied rocks are presented in Table 3. Very important from the point of view of reservoir exploitation are the swelling properties of clastic rocks which depend on total amount of clay minerals and their swelling capacity. Cation exchange capacity (CEC) incorporates both of those rock properties. Thus, it allows for a comprehensive assessment of swelling properties and assignment of the studied rocks to groups with low, medium or high swelling capacity (Stephens et al. 2009).
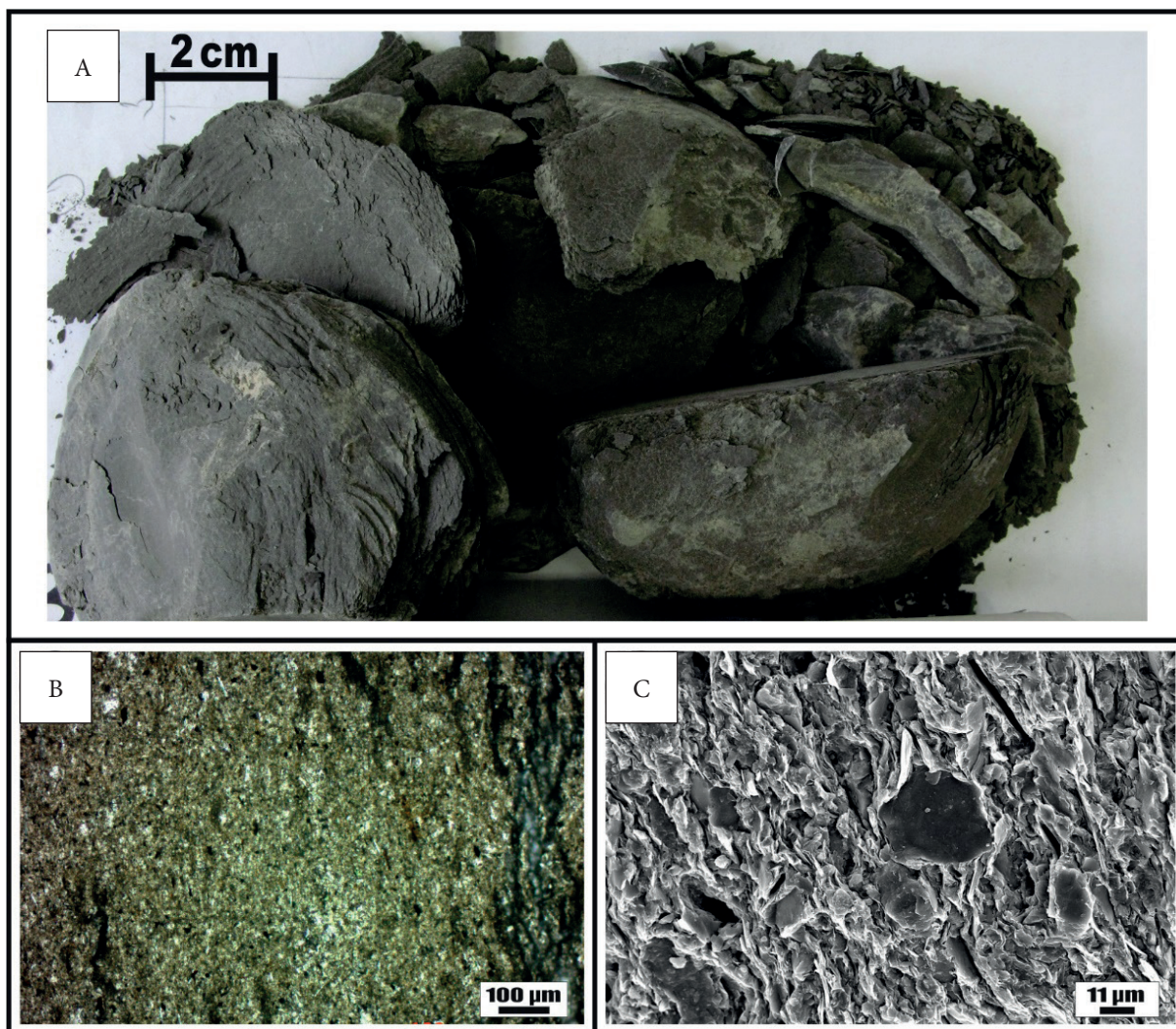

Fig. 16. *Clay shales from the T zone (A); claystone with planar lamination accentuated by alignment of muscovite plates (B); numerous elongated intraparticle micro- and nanopores connected with clay aggregates (C)*

Table 3. *Average quartz, clay minerals and carbonates contents, and CEC values in the distinguished lithotypes*

Zone	Parameter	Lithotype							
		Ss_m	Ss_f	Ss_cl	Ht_s	Ht_sm	Ht_m	Ms	Cs
All samples	Q [%]	52.4	42.4	29.3	33.3	35.6	25.2	22.2	18.8
	Σcl [%]	15.2	26.5	44.0	35.8	35.4	47.2	53.8	58.7
	carbonates [%]	13.1	15.1	14.3	16.8	14.7	17.1	14.3	14.3
	CEC [mval/100g]	3.4	5.6	15.4	12.0	10.0	17.3	18.2	23
S	Q [%]	52.6	38.3	29.3	–	–	24.7	24.4	19.0
	Σcl [%]	17.5	33.0	44.0	–	–	50.7	51.0	58.1
	carbonates [%]	11.2	13.3	14.3	–	–	12.5	14.2	15.3
	CEC [mval/100g]	6.3	7.7	15.4	–	–	17.2	19.1	23.0
T	Q [%]	*52.4*	*45.1*	–	*35.5*	*35.6*	*32.1*	*22.0*	*18.8*
	Σcl [%]	14.0	23.3	–	34.5	35.4	40.4	54.6	58.8
	carbonates [%]	14.0	15.2	–	14.7	14.7	13.9	13.6	14.1
	CEC [mval/100g]	1.9	4.3	–	10.9	10.0	12.8	17.5	23.0
P	Q [%]	–	30.1	–	28.9	–	23.1	20.5	–
	Σcl [%]	–	33.0	–	38.3	–	48.8	54.0	–
	carbonates [%]	–	23.3	–	21.0	–	16.8	17.4	–
	CEC [mval/100g]	–	11.5	–	14.2	–	18.7	20.9	–

Explanations: *Q* – quartz, Σcl – sum of clay minerals, CEC – cation exchange capacity. Ss_m – medium- to fine-grained sandstones, Ss_f – fine- to very fine-grained sandstones, Ss_cl – clayey sandstones, Ht_s – sand-dominated heteroliths, Ht_sm – heteroliths with approx. equal proportions of both lithologies, Ht_m – mud-dominated heteroliths, Ms – mudstones, Cs – clayey shales.

Ss_m lithotype is characterized by the highest average content quartz, and lowest content of clay minerals (Tab. 3). The average content of quartz is similar in both S and T zones, whereas the average clay content is higher in samples from the S zone. The rocks from the S zone display also higher values of cation exchange capacity CEC (Tab. 3).

Ss_f samples from the T zone display a higher quartz content and lower amount of clay minerals than samples from the S zone. The sample from P zone is characterized by the lowest quartz content and the highest amount of carbonates (Tab. 3). As in the case of Ss_m the avg. CEC value is lower in the T region than in the S region (Tab. 3).

Ss_cl lithotype displays much lower Q content and higher clay content than other sandstones. Also, the avg. CEC value is significantly higher (Tab. 3).

As it is in the case of sandstones, **Ht_s** lithotype from the P zone displays lower quartz content, higher clay content, and more carbonates than rocks from the T zone (Tab. 3).

Ht-sm lithotype displays similar values of the measured parameters to Ht_s.

Ht_m litothype is characterized by higher content of clay minerals, lower content of quartz and significantly higher CEC values than other heterolites (Tab. 3). The values of these parameters vary between the studied zones. As it is in the case of Ss_f, Ht_m from the T zone is characterized by the highest amount of quartz, lowest amount of clay minerals and the lowest CEC value (Tab. 3).

Ms lithotype displays similar values of the measured parameters to Ht_m. (Tab. 3). The values are alike in all three zones, the exception being the highest carbonate content in P zone (Tab. 3).

Cs lithotype contains highest amounts of clay minerals, lowest amounts of quartz and highest value of CEC from all the investigated lithotypes.

DISCUSSION

The problem of mineral composition diversity within heterolithic rock complexes (e.g., Peyaud et al. 2010, Virolle et al. 2021, Iqbal et al. 2022), and especially its direct influence on the possibility of reliable determination of the variability of reservoir properties in these formations, have so far been rarely discussed in scientific papers. Many publications are focused mainly on methods of permeability calculations in heterolithic formation profiles (e.g., Norris & Lewis 1991, Jackson et al. 2003, Nordahl et al. 2005, Nordahl & Ringrose 2008), but really the most important problem in heterogeneous reservoir studies is integrating data from different samples, acquired using different test methods (Enderlin et al. 1991, Worthington 1994, Gupta et al. 1996, Corbett et al. 1998, Martinius et al. 2005). A reliable reconstruction of the reservoir properties distribution is possible only on the basis of fully integrated data (Nordahl 2004, Ringrose et al. 2005, Riegel et al. 2019).

The research presented in this paper focused on the integration of different types of data obtained on the basis of macroscopic observations of core materials, petrographic studies in optical and scanning microscopy, mineral (XRD) and chemical (XRF) composition studies, determination of the swelling properties (cation exchange capacity, CEC). The presented results were used in further stage of the study by incorporating them into the interpretation of well logs. The integration of various data obtained by different research methods (and at varying vertical resolution) was aimed at developing the most reliable interpretation of lithology and vertical differentiation of reservoir properties in the whole analyzed intervals of the heterolithic formation (and not only within the intervals covered by cores).

The investigated rocks belong to two distinctly different groups of samples: sand-dominated rocks (Ss_m and Ss_f lithotypes) and mud-dominated rocks, including Ht_m, Ms and Cs lithotypes.

Ss-cl, Ht_s and Ht_sm lithotypes show an intermediate nature, what is implied by interpretation of the correlation diagrams (Figs. 4–7). In all the studied rocks, interlayers of particular lithologies are visible not only in macroscopic scale (sandstone layers from 0.5 mm in the P zone to 3.0 cm in the S zone), but also in microscopic scale, where interlayers of several dozen to several hundred μm are visible.

The differences in the lithology and mineralogy of the distinguished lithotypes are associated basically with varying content of clay minerals and quartz (Figs. 17, 18). The content of clay minerals varies not only between particular lithotypes (avg. clay minerals content increase from Ss_m to Cs) but also regionally. In sand-dominated lithotypes and heteroliths from the T zone the clay content is significantly lower than in other zones. In Ms and Cs lithotypes the clay content is similar in all zones. The Ss_cl lithotype from the S zone is characterized by a much higher content of clay minerals than the other sandstones, mineralogically these rocks are similar to Ht_m, however, there is no distinct layering characteristic for heteroliths. Carbonate minerals in samples from all study zones occur in a similar form of carbonate-clay matrix and crushed bioclasts. The highest carbonate contents were found in the P zone, while no variation in the content of these minerals was observed among the lithotypes (Fig. 19).

Swelling properties of the investigated rocks were defined on the base of the cation exchange capacity CEC values. There is a significant increase in the value of the CEC parameter with decreasing grain size, from less than 1, up to 4 meq/100 g for sandstones (no swelling capacity) to 25 mval/100 g for clayey shales (high swelling capacity) (Fig. 20). As regards differences between particular zones, values for samples from the T zone are usually below average and from the P zone – above (Fig. 20). To sum up, sandstones from T and S zones are characterized by lack of or low swelling capacity (CEC below 10 meq/100 g). Medium swelling properties (CEC from 10 to 20 meq/100 g) are characteristic for Ss_cl, all heteroliths, and Ms from the S and T zones. Ms and Cs from the P zone display high swelling capacity (CEC over 20 meq/100g).
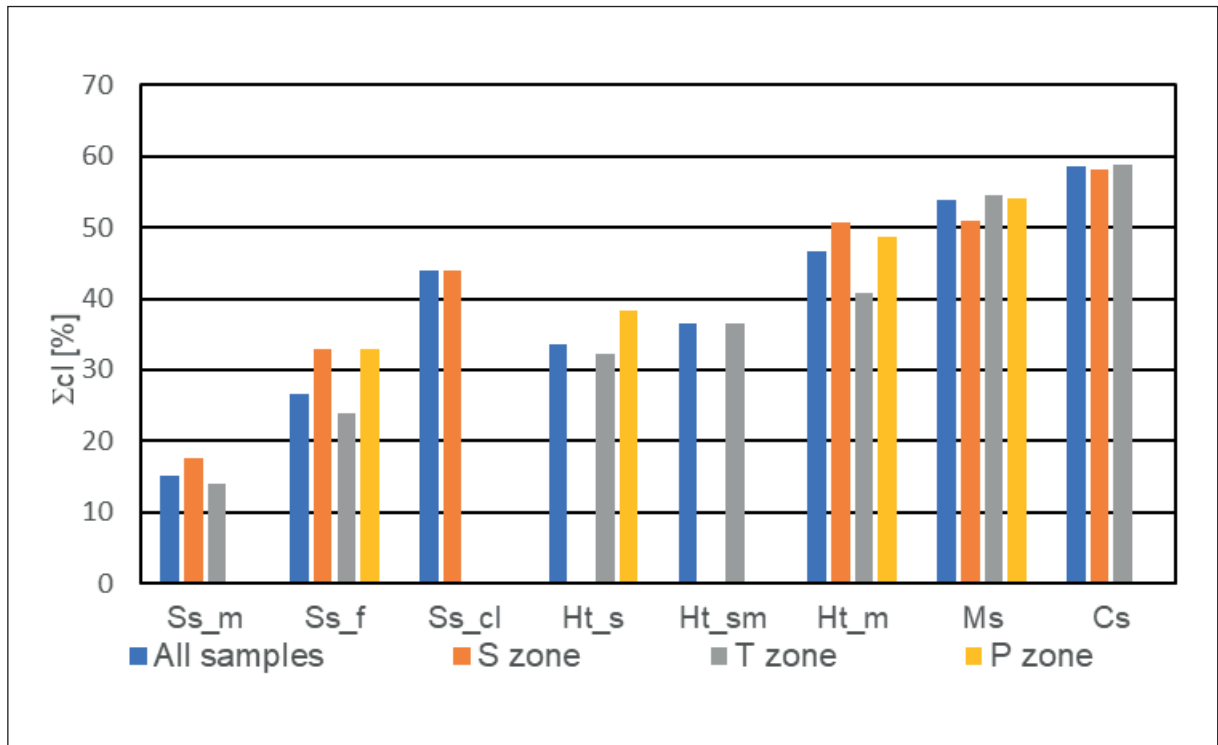
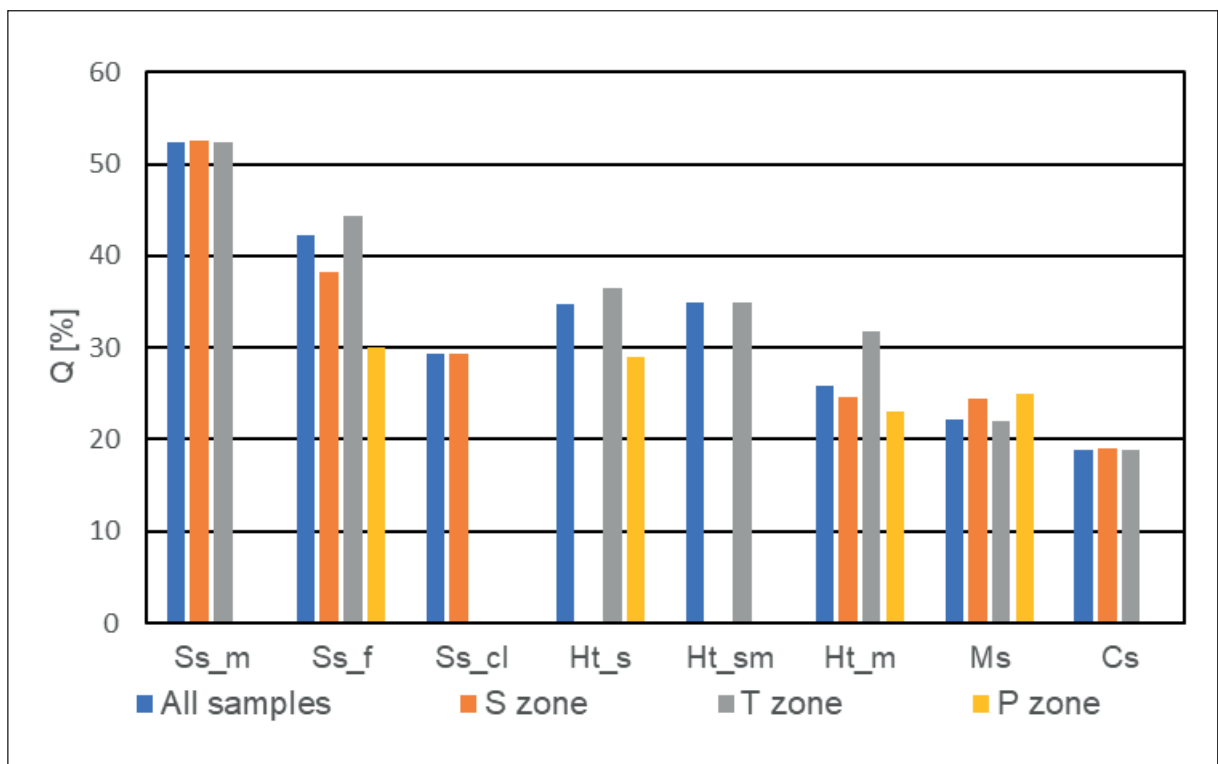**Fig. 17.** *Variability of the clay content (Sum cl) in the separated lithotypes*

Fig. 18. *Variability of the quartz (Q) content in the separated lithotypes*
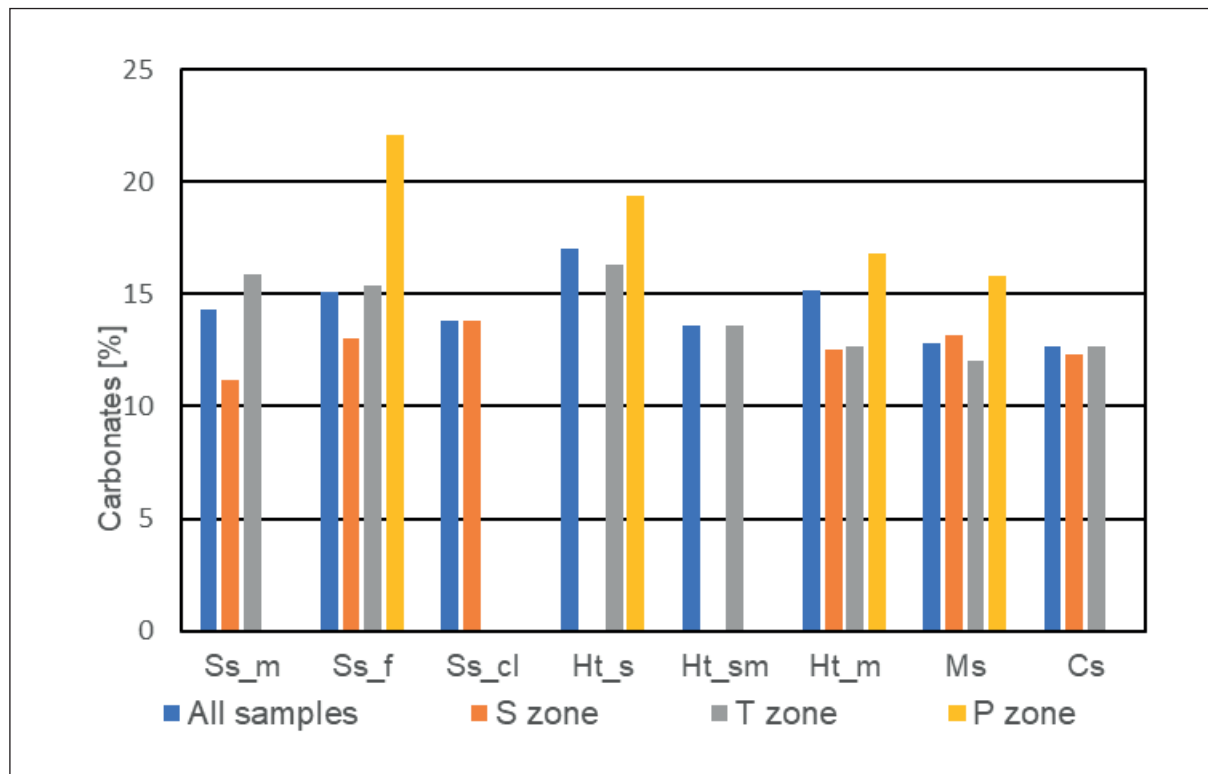
Fig. 19. *Variability of the carbonate (C+D+An) content in the separated lithotypes: C – calcite, D – dolomite, An – ankerite*
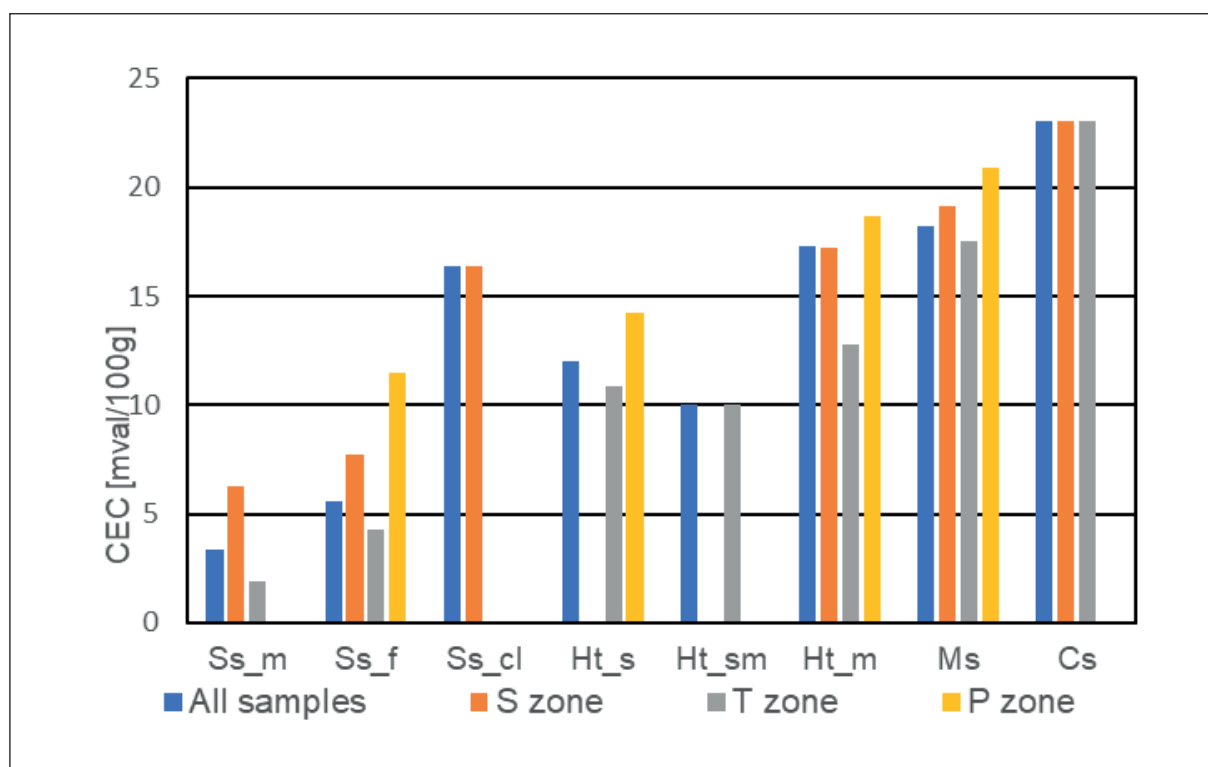

Fig. 20. *Variability of the cation exchange capacity (CEC) content in the separated lithotypes*

It should be emphasized that lithofacial classifications of heterolithic formations are usually based on sedimentological studies, macroscopic and microscope observations (Donselaar & Geel 2007, Siddiqui et al. 2017, Riegel et al. 2019). The presented work was aimed at using macroscopic observations as well as XRD and XRF studies for distinction and characterization of particular lithotypes. The obtained classification proved to be very helpful in the next stage of the project (obtaining reliable average values of petrophysical parameters in the analysed profiles) (Klaja 2019).

The mentioned regional mineralogical differentiation is largely due to the complex palaeogeography of the Middle Miocene Carpathian Foredeep basin and the diversity of the alimentary areas (Studencka 2001, Oszczypko et al. 2006, Kováč et al. 2007). Other important factors influencing the mineralogical differentiation of the Machów Formation heterolithes certainly include various mechanisms of transport and sedimentation (e.g., river and deltaic systems, sedimentation in estuaries, gravity flows, wave processes in the coastal zone), as well as the length of transport of terrigenous material. The above-mentioned factors, together with grain size and sorting, affect not only the variation in mineral composition, but also strongly control porosity and permeability in the siliciclastic rocks (vide Nordahl 2004, Nordahl et al. 2005).

CONCLUSIONS

Eight lithotypes showing differences both in macroscopic features and mineral composition were identified in the Machów Formation heterolithic sediments from three Carpathian Foredeep localities. The division, based on analysis of macroscopic features, was verified by correlation diagrams of mineral (XRD) vs. chemical (XRF) composition data.

Three lithotypes dominate in all the analysed zones: mud-dominated heteroliths, mudstones and fine-grained sandstones. Nevertheless, some characteristic features and differences in mineralogy should be emphasized. The S zone sediments are characterized by the presence of thicker (more than 10 cm) inserts of fine- and medium-grained sandstones characterized by petrophysical parameters

similar to those of conventional reservoir sandstones. Massive mudstone layers are characteristic for the T zone profile. Densely distributed, thin sandstone laminae (order of millimetre size) in mud-dominated heteroliths are typical for the P zone.

Mineralogical heterogenity of the distinguished lithotypes is connected mainly with the varying content of clay minerals and quartz. The boundaries between sandstones and the fine-grained rocks in all the studied zones are generally defined by about 50% quartz and feldspar, 30% of the sum of potassium feldspar and micas and 36% of clay minerals but there are some regional variations. For example, the clay content in sand-dominated lithotypes and heteroliths from the T zone is significantly lower than in the same lithotypes from other zones, and the highest carbonate contents were found in the P zone.

The advantage of the provided correlation diagrams is that they are based on measurements conducted on small amounts of powdered samples (XRD and XRF). Therefore, the presented method can be used in areas in which only drill cuttings are available.

The values of cation exchange capacity CEC clearly indicate significant differences in the swelling capacities of clay minerals, which may be of great importance and should be taken into account in planning of natural gas exploitation from this type of collectors.

Detailed investigations of the heterolithic sequences mineralogical composition as well as description of individual lithotypes provided a basis for precise petrophysical characterization of the analysed profiles. Petrophysical parameters measured in the next stage of the research project were assigned to particular lithotypes what enabled more detailed characterization of the reservoir parameters variability and better correlation of laboratory measurements with geophysical data. Application of the results presented in this paper to interpretation of the well log data enabled to develop reliable lithological models of the Machów Formation clastic sediments profile and, what follows, more precise determination of zones characterized by good reservoir parameters. Results of the mentioned above research are intended to be presented in separate publications.

REFERENCES

AFNOR NFX31-130, 1999. *Qualité des sols – Méthodes chimiques – Détermination de la capacité d'échange cationique (CEC) et des cations extractibles.*

Alexandrowicz S.W., Garlicki A. & Rutkowski J., 1982. Podstawowe jednostki litostratygraficzne miocenu zapadliska przedkarpackiego. *Kwartalnik Geologiczny*, 26, 470–471.

Badics B. & Vető I., 2012. Source rocks and petroleum systems in the Hungarian part of the Pannonian Basin: The potential for shale gas and shale oil plays. *Marine and Petroleum Geology*, 31, 53–69. https://doi.org/10.1016/j.marpetgeo.2011.08.015.

Bardon Ch., 1983. Recommendations pour la détermination experimentale de la capacité d'échange de cations des milieu argileux. *Revue de l'Institut Francais du Petrolé*, 38, 621–626.

Bartha A., Balázs A. & Szalay Á., 2018. On the tectonostratigraphic evolution and hydrocarbon systems of extensional back-arc basins: inferences from 2D basin modelling from the Pannonian basin. *Acta Geodaetica et Geophysica*, 53, 369–394. https://doi.org/10.1007/s40328-018-0225-0.

Craigie N., 2018. Principles of Elemental Chemostratigraphy. A Practical User Guide. *Advances in Oil and Gas Exploration and Production*. https://doi.org/10.1007/978-3-319-71216-1.

Corbett P.W.M., Jensen J.L. & Sorbie K.S., 1998. A review of upscaling and cross-scaling issues in core and log data interpretation and prediction. [in:] Harvey P.K. & Lovell M.A. (eds.), *Core-Log Integration*, Geological Society Special Publication, 136, Geological Society, London, 9–16.

Donselaar C.R. & Geel M.E., 2007. Facies architecture of heterolithic tidal deposits: The Holocene Holland Tidal Basin. *Netherlands Journal of Geosciences*, 86, 389–402. https://doi.org/10.1017/S001677460002360X.

Dudek T. & Środoń J., 1996. Identification of illite/smectite by X-ray powder diffraction taking into account the lognormal distribution of crystal thickness. *Geologica Carpathica Clays*, 5(1), 21–32.

Enderlin M.B., Hansen D.K.T. & Hoyt B.R., 1991. Rock volumes: Considerations for relating well log and core data. [in:] Lake L.W., Carroll H.B. & Wesson T.C. (eds.), *Reservoir Characterization II*, Academic Press, San Diego, 277–288.

Ghosh P., Sarkar S. & Maulik P., 2006. Sedimentology of a muddy alluvial deposit: Triassic Denwa Formation, India. *Sedimentary Geology*, 191, 3–36. https://doi.org/10.1016/j.sedgeo.2013.12.004.

Golonka J. & Picha F. J. (eds.), 2006. *The Carpathians and Their Foreland: Geology and Hydrocarbon Resources*. AAPG Memoir, 84, American Association of Petroleum Geologists, Tulsa, 221–258. https://doi.org/10.1306/985610M843070.

Golonka J., Pietsch K. & Marzec P., 2011. Structure and plate tectonic evolution of the northern Outer Carpathians. [in:] Closson D. (ed.), *Tectonics*, INTECH, Rijeka, Croatia, 65–92.

Gupta R., Johnson H. & Myking B., 1996. Reservoir Characterization of Thinly Laminated Heterolithic Facies within Shallow-Marine Sand Bodies. *AAPG Search and Discovery Article #90951*, AAPG International Conference and Exhibition, Caracas, Venezuela.

Iqbal M.A., Rezaee R., Laukamp C., Pejcic B. & Smith G., 2022. Integrated sedimentary and high-resolution mineralogical characterisation of Ordovician shale from Canning Basin, Western Australia: Implications for facies heterogeneity evaluation. *Journal of Petroleum Science and Engineering*, 208, 109347. https://doi.org/10.1016/j.petrol.2021.109347.

Jackson M.D., Muggeridge A.H., Yoshida S. & Johnson H.D., 2003. Upscaling Permeability Measurements within Complex Heterolithic Tidal Sandstones. *Mathematical Geology,* 35(5), 499–520. https://doi.org/10.1023/A:1026236401104.

Jackson M.D., Yoshida S., Muggeridge A.H. & Johnson H.D., 2005. Three-dimensional reservoir characterization and flow simulation of heterolithic tidal sandstones. *AAPG Bulletin*, 89, 507–528. https://doi.org/10.1306/11230404036.

Jankowski L., 2015. *Nowe spojrzenie na budowę geologiczną Karpat: ujęcie dyskusyjne*. Prace Naukowe Instytutu Nafty i Gazu – Państwowego Instytutu Badawczego, 202, INiG-PIB, Kraków.

Jankowski L., Kopciowski R., Ryłko W., Danysh V., Tsarnenko P.N. & Hnylko O., 2012. Lithostratigraphic correlation of the Outer Carpathian borderlands of Poland, Ukraine, Slovakia and Romania. *Biuletyn Państwowego Instytutu Geologicznego*, 449, 87–98.

Jasionowski M., 1997. Zarys litostratygrafii osadów mioceńskich wschodniej części zapadliska przedkarpackiego. *Biuletyn Państwowego Instytutu Geologicznego*, 375, 43–59.

Király A., Milota K., Magyar I. & Kiss K., 2010. Tight gas exploration in the Pannonian Basin. [in:] Vining B.A. & Pickering S.C. (eds.), *Petroleum Geology: From Mature Basins to New Frontiers: Proceedings of the 7th Petroleum Geology Conference*, Geological Society Petroleum Geology Conference Series, 7(1), 1125, Geological Society, London, 1125–1129. https://doi.org/10.1144/0071125.

Klaja J. (research team leader), 2019. *Opracowanie nowej metodyki dla formacji heterolitowych miocenu zapadliska przedkarpackiego w zakresie badań laboratoryjnych i interpretacji profilowań geofizycznych*. Archive of the Oil and Gas Institute – National Research Institute, Kraków, Poland [unpublished study].

Kotarba M.J., Peryt T.M. & Koltun Y.V., 2011 Microbial Gas system and Prospectives of Hydrocarbon Exploration in Miocene Strata of the Polish and Ukrainian Carpathian Foredeep. *Annales Societatis Geologorum Poloniae*, 81, 523–548.

Kováč M., Nagymarosy A., Oszczypko N., Ślączka A., Csontos L., Marunteanu M., Matenco L. & Márton E., 1998. Palinspastic reconstruction of the Carpathian-Pannonian region during the Miocene. [in:] Rakúš M. (ed.), *Geodynamic development of the Western Carpathians*, Geological Survey of Slovak Republic (GSSR), Bratislava, 189–217.

Kováč M., Andreyeva-Grigorovich A., Bajraktarević Z., Brzobohatý R., Filipescu S., Fodor L., Harzhauser M. et al., 2007. Badenian evolution of the Central Paratethys Sea: paleogeography, climate and eustatic sea-level changes. *Geologica Carpathica*, 58, 579–606.

Kowalska S., 2013. Quantitative analysis of the mineral composition of rocks containing clay minerals by Rietveld method. *Nafta-Gaz*, 69(12), 894–902.

Krzywiec P., Wysocka A., Oszczypko N., Mastalerz K., Papiernik B., Wróbel G., Oszczypko-Clowes M. et al., 2008. Ewolucja utworów mioceńskich zapadliska przedkarpackiego w rejonie Rzeszowa (obszar zdjęcia sejsmicznego 3D Sokołów – Smolarzyny). *Przegląd Geologiczny*, 56(3), 232–244.

Lettley C.D. & Pemberton S.G., 2015. Speciation of McMurray Formation Inclined Heterolithic Strata: Varying Depositional Character Along a Riverine Estuary System. *AAPG Search and Discovery Article #51067(2015)*.

Lis P. & Wysocka A., 2012. Middle Miocene deposits in Carpathian Foredeep: Facies analysis and implications for hydrocarbon reservoir prospecting. *Annales Societatis Geologorum Poloniae*, 82, 239–253.

Łaba-Biel A., Kwietniak A. & Urbaniec A., 2020. Seismic Identification of Unconventional Heterogenous Reservoirs Based on Depositional History – A Case Study of the Polish Carpathian Foredeep. *Energies*, 13, 6036. https://doi.org/10.3390/en13226036.

Maksym A., Baszkiewicz A., Gregosiewicz Z., Liszka B. & Zdanowski P., 2001. Środowiska sedymentacji i właściwości zbiornikowe utworów najwyższej jury i kredy dolnej rejonu Brzezówka-Zagorzyce na tle budowy geologicznej S części zapadliska przedkarpackiego. *Przegląd Geologiczny*, 49(5), 401–407.

Malvić T., 2012. Review of Miocene shallow marine and lacustrine depositional environments in Northern Croatia. *Geological Quarterly*, 56(3), 493–504. https://doi.org/10.7306/gq.1035.

Malvić T., Sučić A., Cvetković M., Resanović F. & Velić J., 2014. Low permeability Neogene lithofacies in Northern Croatia as potential unconventional hydrocarbon reservoirs. *Central European Journal of Geosciences*, 6, 182–194. https://doi.org/10.2478/s13533-012-0168-x.

Martin A.J., 2000. Flaser and wavy bedding in ephemeral streams: A modern and an ancient example. *Sedimentary Geology*, 136, 1–5. https://doi.org/10.1016/S0037-0738(00)00085-3.

Martinius A.W., Ringrose P.S., Brostrøm C., Elfenbein C., Næss A. & Ringås J.E., 2005. Reservoir challenges of heterolithic tidal sandstone reservoirs in the Halten Terrace, mid-Norway. *Petroleum Geoscience*, 11, 3–16.

Matyasik I., Myśliwiec M., Leśniak G. & Such P., 2007. Relationship between Hydrocarbon Generation and Reservoir Development in the Carpathian Foreland (Poland). [in:] Lacombe O., Roure F., Lavé J. & Vergés J. (eds.), *Thrust Belts and Foreland Basins: From Fold Kinematics to Hydrocarbon* Systems, Frontiers in Earth Sciences, Springer, Berlin, Heidelberg, 413–427. https://doi.org/10.1007/978-3-540-69426-7_22.

Moryc W., 1992. Budowa geologiczna podłoża miocenu w rejonie Sędziszów Małopolski – Rzeszów i ich perspektywiczność. *Nafta-Gaz*, 48(9–10), 205–223.

Moryc W., 1996. Budowa geologiczna podłoża miocenu w rejonie Pilzno – Dębica – Sędziszów Małopolski. *Nafta-Gaz*, 52(12), 521–550.

Myśliwiec M., 2004. Mioceńskie skały zbiornikowe zapadliska przedkarpackiego. *Przegląd Geologiczny*, 52(7), 581–592.

Myśliwiec M., Plezia B. & Świętnicka G., 2004. Nowe odkrycia złóż gazu ziemnego w osadach miocenu północno-wschodniej części zapadliska przedkarpackiego na podstawie interpretacji bezpośredniego wpływu nasycenia węglowodorami na zapis sejsmiczny. *Przegląd Geologiczny*, 52(5), 395–402.

Nagymarosy P. & Muller P., 1988. Some Aspects of Neogene Biostratigraphic in the Pannonian Basin. [in:] Royden L.H. & Ferenc Horváth (eds.), *The Pannonian Basin: A Study in Basin Evolution Basin Evolution*, AAPG Memoir, 45, American Association of Petroleum Geologists, Tulsa, 69–77. https://doi.org/10.1306/M45474C6.

Nordahl K., 2004. *A petrophysical evaluation of tidal heterolithic deposits application of a near wellbore model for reconciliation of scale dependent well data*. Norwegian University of Science and Technology, Trondheim.

Nordahl K. & Ringrose P.S., 2008. Identifying the Representative Elementary Volume for Permeability in Heterolithic Deposits Using Numerical Rock Models. *Mathematical Geosciences*, 40, 753–771. https://doi.org/10.1007/s11004-008-9182-4.

Nordahl K., Ringrose P.S. & Wen R., 2005. Petrophysical characterization of a heterolithic tidal reservoir interval using a process-based modelling tool. *Petroleum Geoscience*, 11, 17–28. https://doi.org/10.1144/1354-079303-613.

Norris R.J. & Lewis J.J.M., 1991. The Geological Modeling of Effective Permeability in Complex Heterolithic Facies. *SPE Annual Technical Conference and Exhibition, Dallas, Texas, October 1991*, SPE-22692-MS. https://doi.org/10.2118/22692-MS [conference paper].

Oszczypko N., 2006. Late Jurassic-Miocene evolution of the Outer Carpathian fold-and-thrust belt and its foredeep basin (Western Carpathians, Poland). *Geological Quarterly*, 50(1), 169–194.

Oszczypko N., Krzywiec P., Popadyuk I. & Peryt T., 2006. *Carpathian Foredeep Basin (Poland and Ukraine): Its Sedimentary, Structural, and Geodynamic Evolution*. [in:] Golonka J. & Picha F.J. (eds.), *The Carpathians and Their Foreland: Geology and Hydrocarbon Resources*, AAPG Memoir, 84, American Association of Petroleum Geologists, Tulsa, 239–350. https://doi.org/10.1306/985612M843072.

Pavelić D. & Kovačić M., 2018. Sedimentology and stratigraphy of the Neogene rift-type North Croatian Basin (Pannonian Basin System, Croatia): A review. *Marine and Petroleum Geology*, 91, 455–469. https://doi.org/10.1016/j.marpetgeo.2018.01.026.

Pettijohn F.J., Potter P.E. & Siever R., 1972. *Sand and Sandstone*. Springer, New York. https://doi.org/10.1007/978-1-4615-9974-6.

Peyaud J.B., Bal A., Khalid N.S.B.A. & Diah M., 2010. Improved Methodology for High-Resolution Bed Mineralogy from Wireline Logs. *SPWLA 51st Annual Logging Symposium, Perth, Australia, June 2010*, SPWLA-2010-62460 [conference paper].

Picard M.D., 1971. Classification of fine-grained sedimentary rocks. *Journal of Sedimentary Petrology*, 41, 179–195. https://doi.org/10.1306/74D7221B-2B21-11D7-8648000102C1865D.

Poprawa P., Papiernik B., Krzywiec P., Machowski G. & Maksym A., 2018. Potencjał poszukiwawczy prowincji naftowych w Polsce. *Wiadomości Naftowe i Gazownicze*, 12, 4–12.

Porębski S.J. & Warchoł M., 2006. Znaczenie przepływów hiperpyknalnych i klinoform deltowych dla interpretacji sedymentologicznych formacji z Machowa (miocen zapadliska przedkarpackiego. *Przegląd Geologiczny*, 54(5), 421–429.

Przelaskowska A. & Klaja J., 2014. Cation exchange capacity measurements in sedimentary rocks. *Nafta-Gaz*, 70(7), 432–438.

Riegel H., Zambrano M., Balsamo F., Mattioni L. & Tondi E., 2019. Petrophysical Properties and Microstructural Analysis of Faulted Heterolithic Packages: A Case Study from Miocene Turbidite Successions, Italy. *Geofluids*, 958235929. https://doi.org/10.1155/2019/9582359.

Ringrose P., Nordahl K. & Wen R., 2005. Vertical permeability estimation in heterolithic tidal deltaic sandstones. *Petroleum Geoscience*, 11(1), 29–36. https://doi.org/10.1144/1354-079303-614.

Rzemieniarz A. & Ratuszniak Z., 2008. Nowe spojrzenie na budowę geologiczno-strukturalną utworów miocenu autochtonicznego w rejonie złoża gazu ziemnego Pruchnik-Pantalowice. *Prace Instytutu Nafty i Gazu*, 150, 301–306.

Sacchi M. & Horváth F., 2002. Towards a new time scale for the Upper Miocene continental series of the Pannonian basin (Central Paratethys). *EGU Stephan Mueller Special Publication Series*, 3, 79–94. https://doi.org/10.5194/smsps-3-79-2002.

Siddiqui N.A., Rahman A.H.A., Sum C.W., Yusoff W.I.W. & Ismail M.I., 2017. Shallow-marine sandstone reservoirs, depositional environments, stratigraphic characteristics and facies model: A review. *Journal of Applied Sciences*, 17, 212–237. https://doi.org/10.3923/jas.2017.212.237.

Środoń J., 1980. Precise identification of illite/smectite interstratification by X-ray powder diffraction. *Clays and Clay Minerals*, 28, 401–411. https://doi.org/10.1346/CCMN.1980.0280601.

Środoń J., 1981. X-ray identification of randomly interstratified illite/smectite in mixtures with discrete illite. *Clay Minerals*, 16(3), 297–304. https://doi.org/10.1180/claymin.1981.016.3.07.

Środoń J., 1984. X-ray powder diffraction identification of illitic materials. *Clays and Clay Minerals*, 32, 337–349. https://doi.org/10.1346/CCMN.1984.0320501.

Stephens M., Gomez-Nava S. & Churan M., 2009. Laboratory methods to assess shale reactivity with drilling fluids. *American Association of Drilling Engineers. National Technical Conference & Exhibition, New Orleans, Louisiana, 2009* [conference paper].

Studencka B., 2001. Rekonstrukcje paleogeograficzne Paratetydy w miocenie środkowym: implikacje dla basenu zapadliska przedkarpackiego. *Przegląd Geologiczny*, 49(5), 452–453.

Terwindt J.H.J. & Breusers H.N.C., 1972. Experiments on the Origin of Flaser, Lenticular and Sand-Clay Alternating Bedding. *Sedimentology*, 19, 85–98. https://doi.org/10.1111/j.1365-3091.1972.tb00237.x.

Thomas R.G., Smith D.G., Wood J.M., Visser J., Calverley-Range E.A. & Koster E.H., 1987. Inclined heterolithic stratification – Terminology, description, interpretation and significance. *Sedimentary Geology*, 53, 123–179. https://doi.org/10.1016/S0037-0738(87)80006-4.

Urbaniec A., Stadtmüller M. & Bartoń R., 2019. Possibility of a more detailed seismic interpretation within the Miocene formations of the Carpathian Foredeep based on the well logs interpretation. *Nafta-Gaz*, 75(9), 527–544. https://doi.org/10.18668/NG.2019.09.02.

Urbaniec A., Bartoń R., Bajewski Ł. & Wilk A., 2020. Wyniki interpretacji strukturalnej utworów triasu i paleozoiku przedgórza Karpat opartej na nowych danych sejsmicznych. *Nafta-Gaz*, 76(9), 559–568. https://doi.org/10.18668/NG.2020.09.01.

Velić J., Malvić T., Cvetković M. & Vrbanac B., 2012. Reservoir Geology, Hydrocarbon Reserves and Production in the Croatian part of the Pannonian Basin System Reservoir Geology. *Geologia Croatica*, 65(1), 91–101. https://doi.org/10.4154/GC.2012.07.

Virolle M., Brigaud B., Féniès H., Bourillot R., Portier E., Patrier P., Derriennic H. & Beaufort D., 2021. Preservation and distribution of detrital clay coats in a modern estuarine heterolithic point bar in the Gironde estuary (Bordeaux, France). *Journal of Sedimentary Research*, 91, 812–832. https://doi.org/10.2110/jsr.2020.146.

Worthington P.F., 1994. Effective integration of core and log data. *Marine and Petroleum Geology*, 11(4), 457–466. https://doi.org/10.1016/0264-8172(94)90079-5.